JGS
Journal of the Geological Society

Research article

Published online March 21, 2017 https://doi.org/10.1144/jgs2016-080 | Vol. 174 | 2017 | pp. 759–772

Zircon U–Pb age and Hf isotope evidence for an Eoarchaean crustal remnant and episodic crustal reworking in response to supercontinent cycles in NW India

Wei Wang[1,2*], Peter A. Cawood[3,4], Manoj K. Pandit[5], Mei-Fu Zhou[2] & Wei-Terry Chen[6]

[1] State Key Laboratory of Geological Processes and Mineral Resources, School of Earth Sciences, China University of Geosciences, Wuhan 430074, China
[2] Department of Earth Sciences, The University of Hong Kong, Hong Kong, Hong Kong SAR, China
[3] School of Earth, Atmosphere & Environment, Monash University, Melbourne, VIC 3800, Australia
[4] Department of Earth Sciences, University of St Andrews, North Street, St Andrews KY16 9AL, UK
[5] Department of Geology, University of Rajasthan, Jaipur 302004, Rajasthan, India
[6] State Key Laboratory of Ore Deposit Geochemistry, Institute of Geochemistry, Chinese Academy of Sciences, Guiyang 550002, China

W.W., 0000-0002-7944-7598
* Correspondence: wwz@cug.edu.cn

Abstract: Scattered T_{DM2} (3.8 – 3.2 Ga) for 3.28 – 2.99 Ga zircons from the Proterozoic Delhi Supergroup in northwestern India provide evidence for generation of juvenile crust and reworking of older crust. Depleted mantle-like $\varepsilon_{Hf(t)}$ values (+7.2 to +5.6) for 2.86 – 2.71 Ga zircons indicate that generation of juvenile crust occurred during this period and ceased at 2.71 Ga. Extensive magmatism at 2.66 – 2.34, 2.11 – 2.01 and 1.60 – 1.37 Ga was dominated by reworking of pre-existing crust with variable ages, and the last two periods were accompanied by formation of juvenile crust. An Eoarchaean age of 3671 ± 15 Ma represents the oldest age found in NW India. Zircons formed during supercontinent assembly have positive to negative $\varepsilon_{Hf(t)}$ values, suggesting involvement of juvenile and ancient crust, whereas largely positive $\varepsilon_{Hf(t)}$ values for zircons crystallized subsequent to supercontinent amalgamation suggest involvement of predominantly juvenile crust. Correlation of detrital age patterns and tectonomagmatic events indicates a conjugate position for northern Indian and the Cathaysia Block of South China during the assembly of Nuna. The South China Block remained juxtaposed to India until its separation from Pangaea in the late Palaeozoic.

Supplementary material: Supplementary data, including detailed metadata related to laboratory and sample preparation methods, U-Pb and Lu-Hf isotopic compositions of the analyzed samples and standards are available at https://doi.org/10.6084/m9.figshare.c.3711847

Received 7 July 2016; **revised** 7 February 2017; **accepted** 8 February 2017

The physicochemical resilience of zircon, which is present as an accessory mineral in the majority of igneous, metamorphic and sedimentary rocks, along with advances in micro-analytical techniques allowing rapid determination of zircon's chemical character, have provided important new data to enhance understanding of continental growth and palaeogeography (Amelin *et al.* 1999; Wilde *et al.* 2001; Cawood *et al.* 2007, 2013*a*; Dhuime *et al.* 2012). Zircon ages and Hf-isotopic data have proved particularly valuable in inferring the evolution of the early Earth where significant gaps punctuate the rock record and preserved material is often strongly reworked by younger events (e.g. Harrison 2009; Kemp *et al.* 2010; Reimink *et al.* 2014, 2016, Xing *et al.* 2016). In particular, detrital zircons derived from magmatic and metamorphic sources can provide insights into source regions that either are no longer preserved or have been structurally removed (e.g. Cawood *et al.* 2012).

Peninsular India assembles a collage of ancient cratonic nuclei that formed and stabilized during the Archaean to Palaeoproterozoic (Meert & Pandit 2015). Nevertheless, except for a 3.63 Ga detrital zircon from the Older Metamorphic Group metasedimentary rocks from the Singhbhum Craton in eastern India (Mishra *et al.* 1999), no direct evidence has so far been found for the existence of Eoarchaean or earlier crustal components. However, Hf isotopes of some zircons suggested that formation of Hadean and Eoarchaean crust occurred extensively in the South India Block (Santosh *et al.* 2016). Furthermore, northern India is crucial in reconstructing the Great India Shield in Precambrian supercontinent cycles, although debate surrounds its position with respect to other continental blocks (Rogers & Santosh 2002; Zhao *et al.* 2002; Kaur *et al.*, 2013; Cawood *et al.* 2013*b*).

In this paper, we report U–Pb and Hf isotopic data from detrital zircons of the Proterozoic Delhi Supergroup, northwestern Peninsular India, to demonstrate inputs from source regions that record a protracted history of crustal growth and reworking. These data are then used to demonstrate how the history of the sedimentary source can be used to constrain the palaeogeography of the region from the Archaean to the Mesoproterozoic, during the Nuna and Rodinia supercontinent cycles.

Precambrian geology of NW India

Peninsular India is a collage of five Archaean cratonic nuclei: the Banded Gneiss Complex and the Bundelkhand, Singhbhum, Bastar and Dharwar cratons, which are thought to have stabilized during Archaean to Palaeoproterozoic times (3.8 – 1.6 Ga) (Meert & Pandit 2015). The Banded Gneiss Complex occupies the northwestern part of Peninsular India and includes a Palaeo- to Neoarchaean basement comprising granitic gneisses, migmatites, metadolerite (amphibolites)

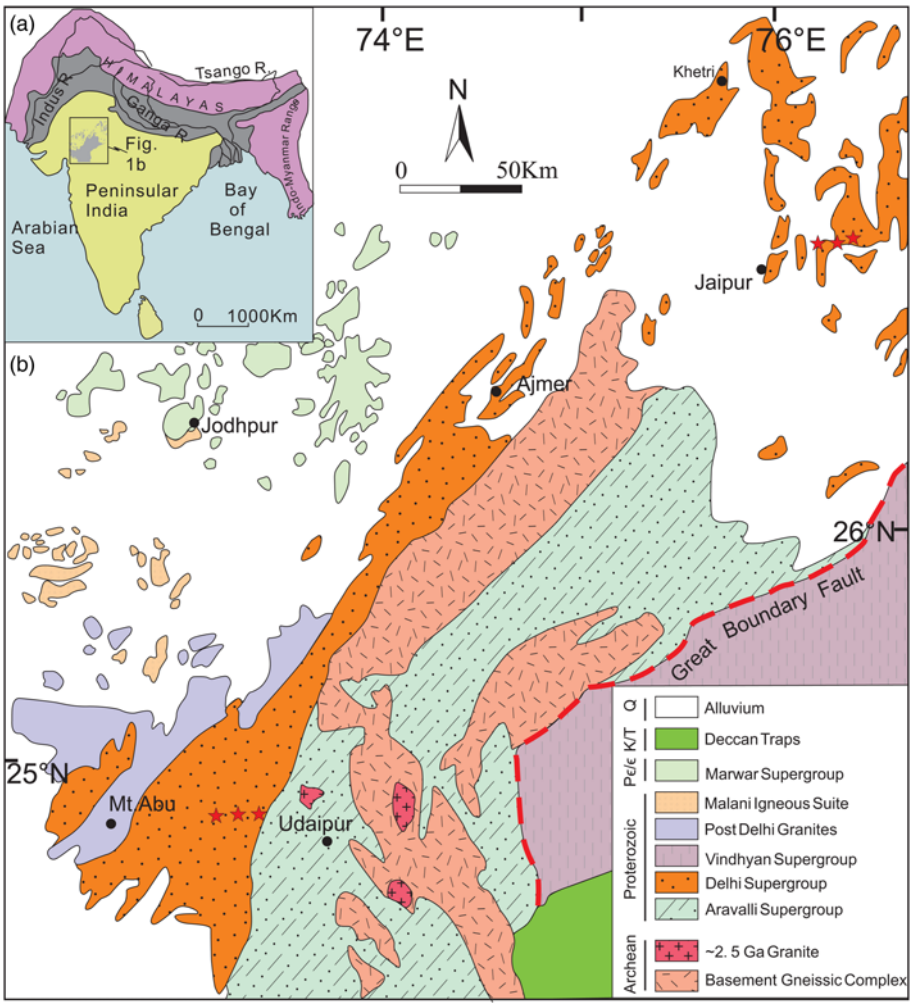

Fig. 1. (**a**) Map showing disposition of Aravalli–Delhi Fold Belt in northwestern India; (**b**) simplified geological map of the Aravalli–Delhi Fold Belt showing distribution of major Precambrian lithotectonic units (modified after Roy & Jakhar 2002). Asterisks represent the sample locations.

and intrusive granitoids with minor metavolcanic and metasedimentary rocks (Heron 1953). The oldest rock units in the region are amphibolite-facies trondhjemite–tonalite–granodiorite gneisses (TTG), and have yielded *c.* 3.3 and 2.5 Ga U–Pb igneous zircon ages (Wiedenbeck & Goswami 1994; Roy & Kröner 1996; Wiedenbeck *et al.* 1996). The *c.* 2.5 Ga Berach Granite marks stabilization of the Archaean crust in this region. The Banded Gneiss Complex also forms the basement for the unconformably overlying Proterozoic Aravalli and Delhi supracrustal sequences (metasedimentary and metavolcanic rocks). The Aravalli Supergroup, of presumed Palaeoproterozoic age, is exposed in the southern part of the Aravalli–Delhi Fold Belt, whereas the younger (Meso- to Neoproterozoic) Delhi Supergroup forms the dominant lithostratigraphic unit of the >750 km long NE–SW-trending Aravalli mountains (Fig. 1). The contact between the Aravalli and Delhi supergroups is sheared and equivocally described, either as an unconformity (Heron 1953) or as a suture representing the closure of the Proterozoic Aravalli ocean (Sugden *et al.* 1990).

Delhi Supergroup

The Delhi Supergroup unconformably overlies the Banded Gneiss Complex (Fig. 2a) and consists of clastic and chemical metasedimentary and minor metavolcanic rocks (Gupta *et al.* 1980; Gupta 1997). They are tightly folded into a regional synclinorium (Heron 1953) as a result of multiple deformation episodes. Rocks from the Delhi Supergroup have undergone upper greenschist- to amphibolite-facies metamorphism. Heron (1953) proposed subdivision of the Delhi Supergroup (system) into an older Alwar Group (series) and younger Ajabgarh Group (series), with the Raialo Group (series) as an independent chronostratigraphic unit between the Aravalli and Delhi supergroups (Fig. 3). In a major revision, based on the new stratigraphic code of nomenclature, Gupta *et al.* (1980) proposed inclusion of the Raialo Group (quartzite, carbonate and mafic volcanic rocks) as the lowermost unit of the Delhi Supergroup, followed by the Alwar (predominantly arenite) and Ajabgarh (argillite- and carbonate-facies) groups (Fig. 2b and c). Delhi rocks are geographically distributed in the northeastern and southwestern domains of the Aravalli–Delhi Fold Belt. The northeastern domain is further subdivided from east to west into the Bayana–Lalsot, Alwar and Khetri sub-basins. Although retaining the basic stratigraphy of Heron (1953) for the northeastern segment, Gupta *et al.* (1980) introduced the term Gogunda Group (equivalent to the Alwar Group) for the lower unit of the Delhi Supergroup in the southwestern domain. The Gogunda Group comprises dominant quartzite (at times arkosic), schist and metaconglomerate (Fig. 2d). These rocks are overlain by calc-siltstone, quartzite, schist, gneiss and carbonate-bearing rocks of the Kumbhalgarh Group (equivalent to the Ajabgarh Group) (Fig. 2e and f).

Sampling and analytical methods

For this study, six samples (five quartzites and one meta-calcic siltstone) of the Delhi Supergroup including three each from the northeastern and southwestern domains, as well as a basement granite–gneiss sample (DLW1401), were analysed. Sample locations are shown in Figure 1 and global positioning system (GPS) coordinates are given in the supplementary material. Approximately 2 kg of each sample was processed for zircons using standard heavy mineral separation procedures.

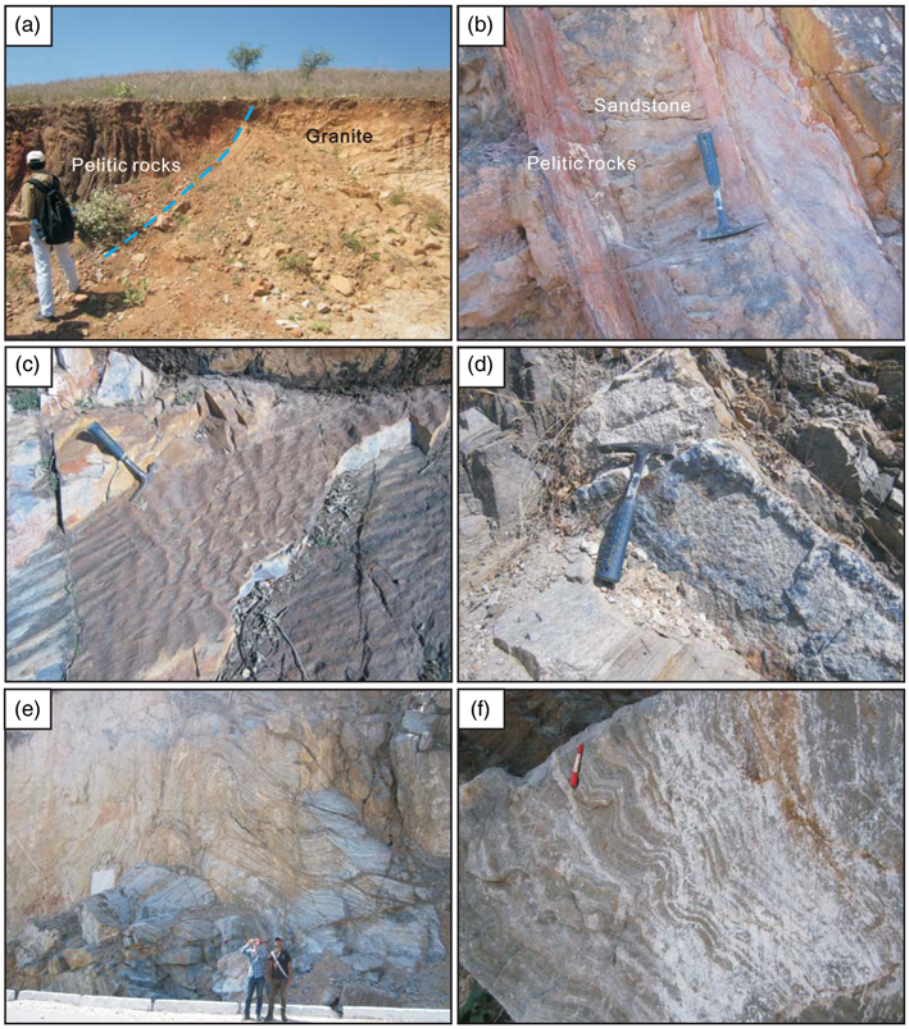

Fig. 2. Field photographs showing the outcrop features of the Northern Delhi Supergroup: (**a**) pelitic rocks of the Raialo Group unconformably overlying Archaean granite; (**b**) massive grey arenitic rocks with thin layer of reddish pelitic rocks, Alwar Group; (**c**) straight ripple marks are truncated at right angles by sinuous ripple marks. Southern Delhi Supergroup: (**d**) pegmatitic quartz vein in Gogunda quartz sandstone; (**e**) strongly folded interbedded siliciclastic and carbonaceous rocks; (**f**) folded carbonate rocks with recrystallized calcite in the friction surface, Kumbhalgarh Group.

Morphology and internal structure of zircon separates were observed using a Gatan Mono CL 4+ detector attached to a FEI Quanta 450 FEG in the State Key Laboratory of Geological Processes and Mineral Resources (SKLGPM). Cathodoluminescence (CL) images were used to select target portions of zircon grains with clear growth zoning for spot analysis, avoiding inherited cores, inclusions and fractures. Selected zircons were subjected to *in situ* U–Pb and Lu–Hf isotopic analyses using an Agilent 7500a inductively coupled plasma mass spectrometry (ICP-MS) system and a Neptune Plus multi-collector (MC)-ICP-MS system, both coupled to a 193 nm ArF excimer laser ablation system, housed at the SKLGPM, China University of Geosciences, Wuhan. The Geolas 193 nm ArF excimer laser, homogenized by a set of beam delivery systems, was focused on the zircon surface with a fluence of 8 J cm^{-2}. A spot diameter of 32 μm was ablated at 5 Hz repetition rate for 45 s. Helium (optimized to obtain the highest sensitivity) was applied as a carrier gas to allow efficient transportation of aerosol to the ICP-MS system using a 1 m transfer tube with an internal diameter of 3 mm. Zircon 91500 was used as the primary standard to correct elemental fractionation, and zircon GJ-1 (Jackson *et al.*, 2004) was analysed as the unknown sample for quality control. Raw data reduction was performed off-line by *ICPMSDataCal* (Liu *et al.* 2010) and the results were reported with 2σ errors. Reported uncertainties (2σ) of the $^{206}Pb/^{238}U$ ratio were propagated by quadratic addition of the external reproducibility (2 SD%) of standard zircon 91500 during the analytical session and the within-run precision of each analysis (2 SE%; standard error) (Liu *et al.* 2010). Because the net intensities of 204 (Pb + Hg) are lower than 20 c.p.s. in most cases, common Pb was not subtracted in this work owing to the large analytical uncertainty. Data were processed using the ISOPLOT and DensityPlotter programs (Ludwig 2003; Vermeesch 2012). The concordant age of analysed GJ-1 (601 ± 17 Ma, 2σ, MSWD = 1.3, n = 22) is consistent with the recommended value (GJ-1: 599.8 ± 1.7 Ma, 2σ; Jackson *et al.*, 2004). Detailed metadata related to the laboratory and sample preparation methods, following the guideline of Horstwood *et al.* (2016), and analytical results for reference materials and samples are given in the supplementary material.

Hf isotopes were obtained with a beam diameter of 55 μm, pulse rate of 10 Hz and energy density of 15 J cm^{-2}. Helium was applied as carrier gas to efficiently transport aerosol to the MC-ICP-MS system. Atomic masses 172 – 179 were simultaneously measured in a static-collection mode. Isobaric interference of ^{176}Yb with ^{176}Hf was corrected against the $^{176}Yb/^{172}Yb$ ratio of 0.5887 (Wu *et al.* 2006). The interference of ^{176}Lu on ^{176}Hf is not considered because of the extremely low $^{176}Lu/^{177}Hf$ ratios in zircons (normally <0.002). Instrumental mass bias corrections of Yb isotope ratios were normalized to $^{172}Yb/^{173}Yb$ of 1.35274 (Chu *et al.* 2002) and Hf isotope ratios to $^{179}Hf/^{177}Hf$ of 0.7325 (Patchett *et al.* 1981) using an exponential law. Owing to insignificant contribution of signal intensity of ^{176}Lu on ^{176}Hf (generally <1%), the mass bias of Lu isotopes (β_{Lu}) can be assumed to be identical to β_{Hf} (see Iizuka & Hirata 2005). Zircon standard 91500 was used for quality control. GJ-1 and TEM were analysed as unknown samples during the analyses to evaluate the reliability of the analytical data. Mean $^{176}Hf/^{177}Hf$ values for 91500, GJ-1 and TEM are 0.282314 ± 35 (n = 37, 2SD), 0.282017 ± 48 (n = 8, 2SD) and 0.2582695 ± 35 (n = 8, 2SD), respectively. Decay constant of 1.867×10^{-11},

$^{176}Hf/^{177}Hf_{CHUR} = 0.282772$, $^{176}Hf/^{177}Hf_{CHUR} = 0.0332$, $^{176}Lu/^{177}Hf_{DM} = 0.0384$ and $^{176}Hf/^{177}Hf_{DM} = 0.283251$ for the Chondritic Uniform Reservoir (CHUR) and Depleted Mantle (DM) (Blichert-Toft & Albarède 1997; Griffin *et al.* 2000; Söderlund *et al.* 2004) were employed in calculating the values of $\varepsilon_{Hf(t)}$, T_{DM} and $f_{Lu/Hf}$.

Results

U–Pb isotope and Lu–Hf isotope analytical data are presented in the supplementary material. Typical CL images of zircons are presented in Figure 4. All U–Pb data are plotted on concordia diagrams (Figs 5 and 6) and detrital zircons with concordant ages (degree of concordance between 90 and 110%) are used for interpretations.

Sample DLW1401, basement granite underlying the Raialo Group

Sample DLW1401 is a granite collected from the basement just below the contact with the overlying Raialo Group (Fig. 2a). The granite predominantly consists of quartz, plagioclase and alkali feldspar with minor muscovite, and accessory zircon and apatite. Alkali feldspar grains are partly altered to kaolinite. Some zircons from this sample consist of an oscillatory zoned core mantled by dark uniform rims, whereas some others show low-luminance features with uniform or unclear zoning structures (Fig. 5). All 18 analyses are discordant with a poorly defined discordia line that has an upper intercept at 2968 ± 220 Ma ($n = 18$, MSWD = 9). Twelve analyses on oscillatory cores, with Th/U ratios of 1.25 – 0.04, yield a discordia line with an upper intercept at 2985 ± 49 Ma and an lower intercept at −98 ± 190 Ma ($n = 12$, MSWD = 0.67), whereas the other six analyses on low-luminance zircons have lower Th/U ratios (0.54 – 0.03) that deviated from this discordia line (Fig. 5). Thus, *c.* 2985 Ma is considered to represent the crystallization age of the granite.

Quartzite from the Raialo Group, sample DLW1404

Raialo Group quartzite sample DLW1404 is from the northern Delhi Supergroup and was collected from a few metres above the contact with the basement. Zircons in this sample are subhedral to subrounded and show well-preserved uniform oscillatory zoning (Fig. 4a). The Th/U ratios range from 1.21 to 0.20, suggesting an igneous origin. Nearly one-third of all the analyses gave discordant U–Pb ages, suggestive of lead loss from these zircons after crystallization. The sample contains a predominant population of late Archaean to early Palaeoproterozoic (2532 ± 27 to 2309 ± 30 Ma) zircon grains with an age peak at *c.* 2.51 Ga (Fig. 7a). The youngest $^{207}Pb/^{206}Pb$ age of 2309 ± 30 Ma (Fig. 7a) constrains the maximum depositional age of the Raialo Group. Constraining maximum depositional age based on a single grain has limitations (Spencer *et al.* 2016), but the angular shape of this grain suggests minimal transport and is different from the subrounded morphology of slightly older grains (2369 ± 38 and 2376 ± 29 Ma, and Fig. 4a). Moreover, the youngest grain shows uniform oscillatory zoning and has a degree of concordance of 97.1%, precluding mixing of two isotopic zones. All zircons from DLW1404 have subchondritic $\varepsilon_{Hf(t)}$ values (−0.1 to −5.3) (Fig. 8a), corresponding to two-stage hafnium model ages (T_{DM2}) of 3.3 – 3.0 Ga.

Quartzite from the Alwar Group, sample DLW1411

Sample DLW1411 is a quartzite from the Alwar Group, collected from the northern Delhi Supergroup. It contains subhedral to subrounded zircon grains with typical oscillatory zoning and a uniform internal structure (Fig. 4b). Late Archaean to early Palaeoproterozoic zircon grains with an age peak at *c.* 2.52 Ga are the dominant population in this sample (Fig. 7b). A single zircon grain yielded a $^{207}Pb/^{206}Pb$ age of 3671 ± 15 Ma, which is the oldest age reported from NW India. This grain is subhedral and shows well-preserved oscillatory zoning (Fig. 4b). Th/U ratio of 0.98 implies an igneous origin. The youngest single zircon grain has a $^{207}Pb/^{206}Pb$ age of 2110 ± 33 Ma with degree of concordance of 100.6% (Fig. 7b). This youngest grain shows a uniform internal structure that is different from the oscillatory zoning of older grains (2350 ± 24 and 2485 ± 17 Ma, Fig. 4b). Other zircons that deviate from the major age peak have ages of 3070 – 2980 Ma ($n = 4$), 2808 – 2683 Ma ($n = 4$) and 2350 ± 24 Ma. Four analyses gave reverse discordant ages but low contents of U (224 – 32 ppm) and probably reflect inhomogeneous Pb distribution (see Kusiak *et al.* 2013).

The oldest zircon has an $\varepsilon_{Hf(t)}$ value of +0.1 and T_{DM2} of 3.9 Ga. Two zircon grains with $^{207}Pb/^{206}Pb$ ages of 2808 ± 23 and 2709 ± 30 Ma have depleted mantle-like $\varepsilon_{Hf(t)}$ values of +5.6 and +6.6, corresponding to T_{DM2} of 2.9 and 2.8 Ga, respectively, close to their $^{207}Pb/^{206}Pb$ ages (Fig. 8a). Late Archaean to early Palaeoproterozoic zircon grains have highly variable $\varepsilon_{Hf(t)}$ values (+5.1 to −9.0, 90% being negative) and T_{DM2} (3.6 – 2.8 Ga). The youngest zircon has the lowest $\varepsilon_{Hf(t)}$ value of −12.1 with T_{DM2} of 3.6 Ga, close to the oldest age of 3.67 Ga.

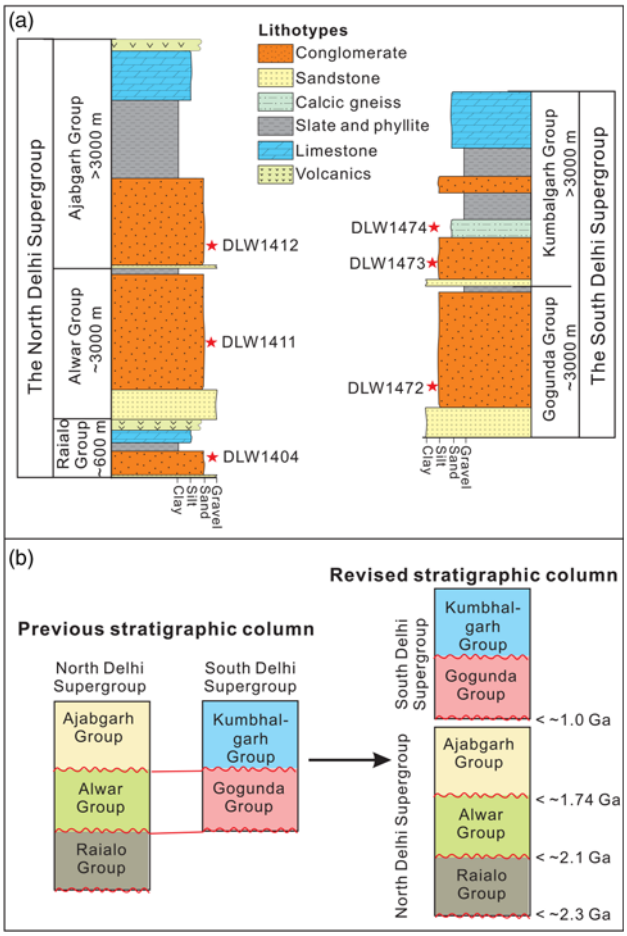

Fig. 3. Representative lithostratigraphic column of the North and South Delhi Supergroups (modified after Gupta *et al.* 1980; Roy & Jakhar 2002). Proposed stratigraphic correlation for the North and South Delhi Supergroups is also shown.

Quartzite from the Ajabgarh Group, sample DLW1412

Sample DLW1412 was collected from the Ajabgarh Group in the northern Delhi Supergroup (Fig. 1). Most zircon grains in this sample are rounded to subrounded, and CL images reveal patterns

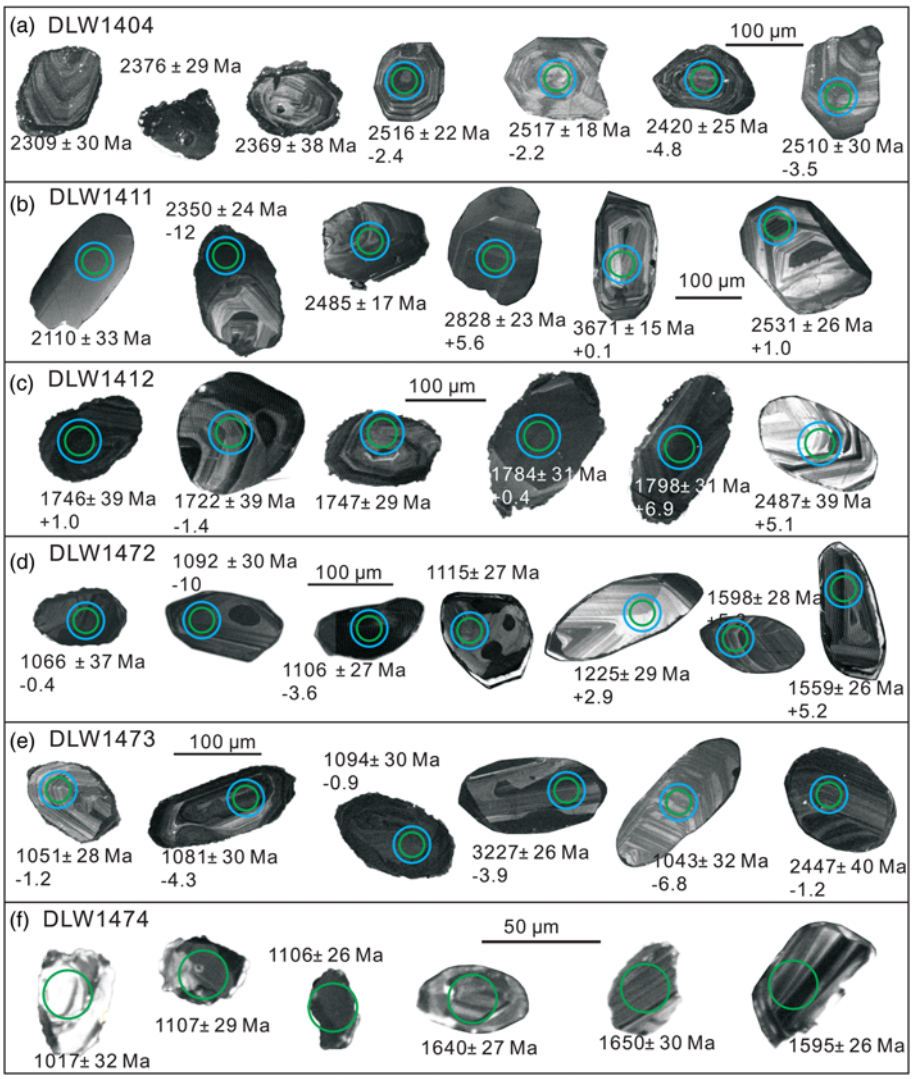

Fig. 4. Cathodoluminescence (CL) images showing external morphology and internal structure of analysed zircon grains.

varying from oscillatory zoning to homogeneous (unzoned) dark luminescence (Fig. 4c). All the analyses are concordant with $^{207}Pb/^{206}Pb$ ages ranging from 3298 ± 11 to 1722 ± 39 Ma and Th/U ratios from 1.78 to 0.12, and most ages are between 2166 and 1722 Ma with a major age peak at *c.* 1.88 Ga and a subordinate peak at *c.* 2.53 Ga (Fig. 7c). The youngest three zircon grains (1722 ± 39, 1746 ± 39 and 1747 ± 29 Ma) show rounded morphology with well-preserved oscillatory zoning, different from the elongated grains of slightly older zircons (1784 ± 31 and 1798 ± 31 Ma, Fig. 4c). Therefore, the weighted mean $^{207}Pb/^{206}Pb$ age of 1740 ± 39 Ma (MSWD = 0.14, 2σ) for the three youngest ages can regarded as the maximum depositional age of the Ajabgarh sandstone.

The three oldest zircon grains (3.28 – 3.06 Ga) from the sample have $\varepsilon_{Hf(t)}$ values between +0.3 and −1.8, and T_{DM2} of 3.6 – 3.4 Ga. Late Archaean to early Palaeoproterozoic zircon grains have highly variable $\varepsilon_{Hf(t)}$ values (+5.1 to −5.3) and T_{DM2} (3.4 – 2.6 Ga). Scatter in Hf isotopic ratios is observed among the Palaeoproterozoic population ($\varepsilon_{Hf(t)}$ values +6.9 to −22.8, T_{DM2} 3.8 – 2.0 Ga) (Fig. 8a). The lowest $\varepsilon_{Hf(t)}$ value of −22.8 corresponds to a T_{DM2} of 3.8 Ga, similar to the T_{DM2} (3.9 Ga) of the oldest zircon in the Alwar quartzite sample (DLW1411).

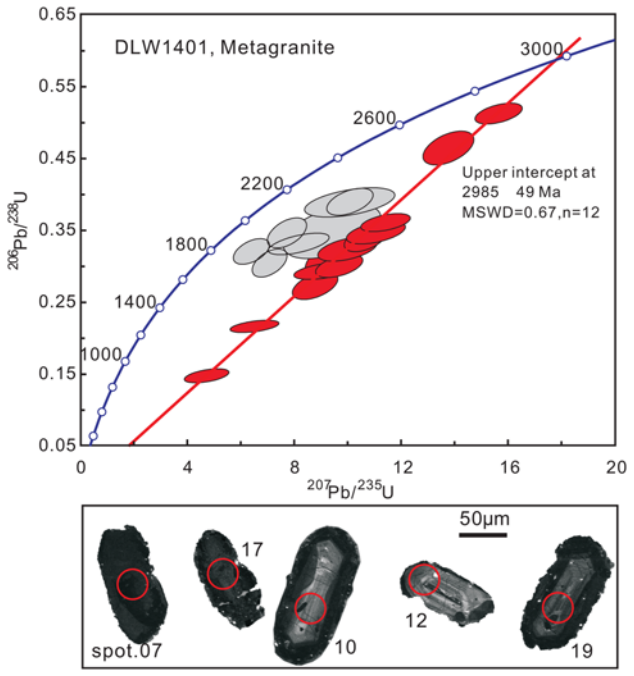

Fig. 5. Concordia plots with CL images of zircons for the basement granite of the northeastern domain of the Delhi Supergroup. Spot number of analysis is shown.

Quartzite from the Gogunda Group, sample DLW1472

Sample DLW 1472 is a quartzite from the southwestern segment of the Delhi Supergroup, collected from a road section west of Udaipur city. Most zircon grains in this sample are rounded to subrounded

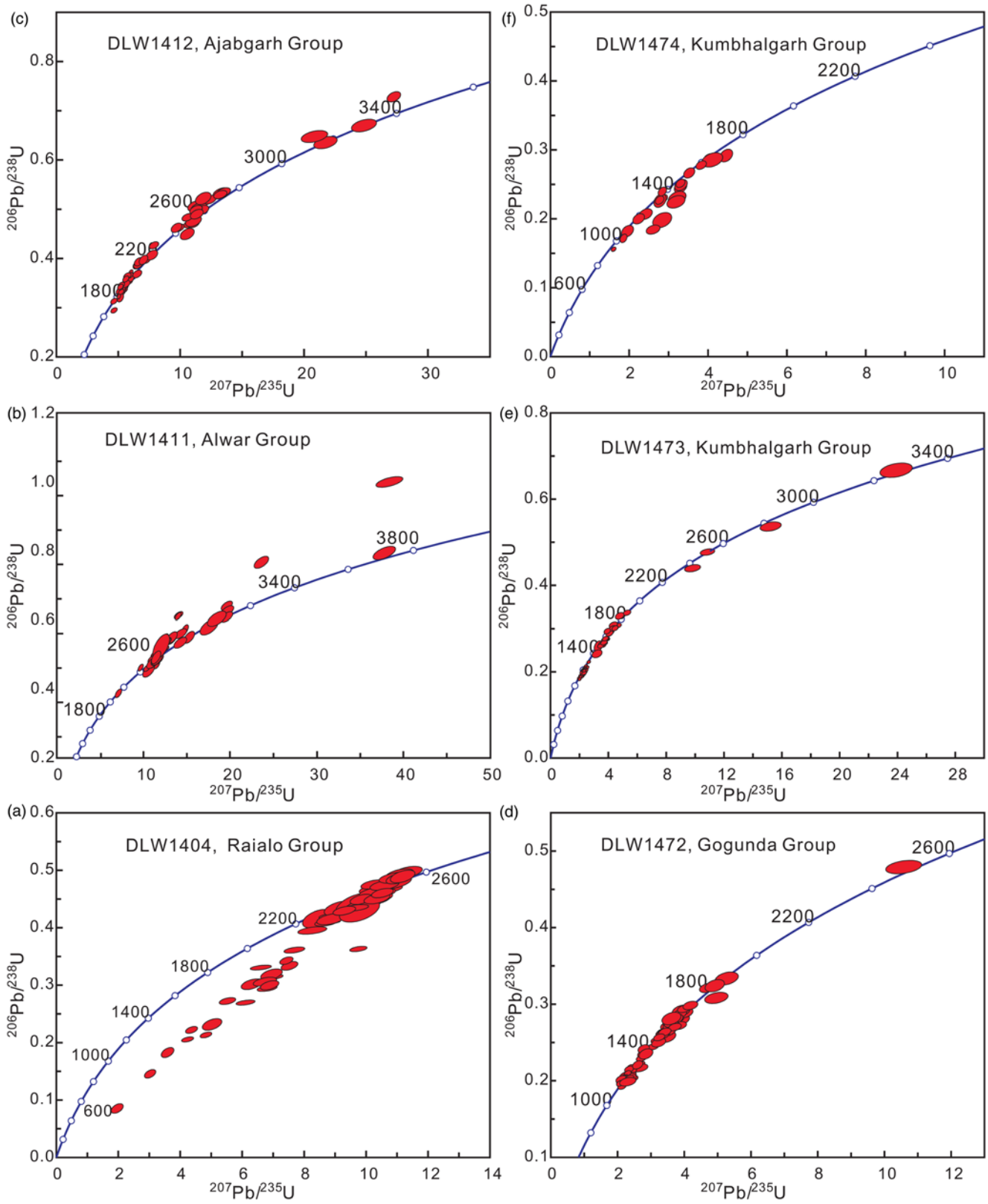

Fig. 6. Concordia plots of zircons for sedimentary rocks from the northeastern segment of the Delhi Supergroup, northwestern India.

with a subordinate population of euhedral grains (Fig. 4d). Some of the grains display oscillatory zoned cores mantled by thin overgrowths (Fig. 4d). Zircons in this sample are predominantly late Palaeoproterozoic to Mesoproterozoic with $^{207}Pb/^{206}Pb$ ages ranging from 1717 ± 37 to 1066 ± 37 Ma and forming a major peak at *c.* 1.48 Ga (Fig. 7d). Three reverse discordant analyses have variable U contents (1355 – 363 ppm) that are unrelated to the degree of discordance, suggesting that patchy distribution of Pb was the likely cause for their reverse discordance (Kusiak *et al.* 2013). All the concordant analyses yield Th/U ratios in the range of magmatic zircons (3.23 – 0.23), except for a single grain with Th/U ratio of 0.09 and $^{207}Pb/^{206}Pb$ age of 1124 ± 38 Ma. The subrounded youngest zircon grain (spot 60, 1066 ± 37 Ma) shows a dark, ambiguous core with a very thin light rim, which is similar to spot

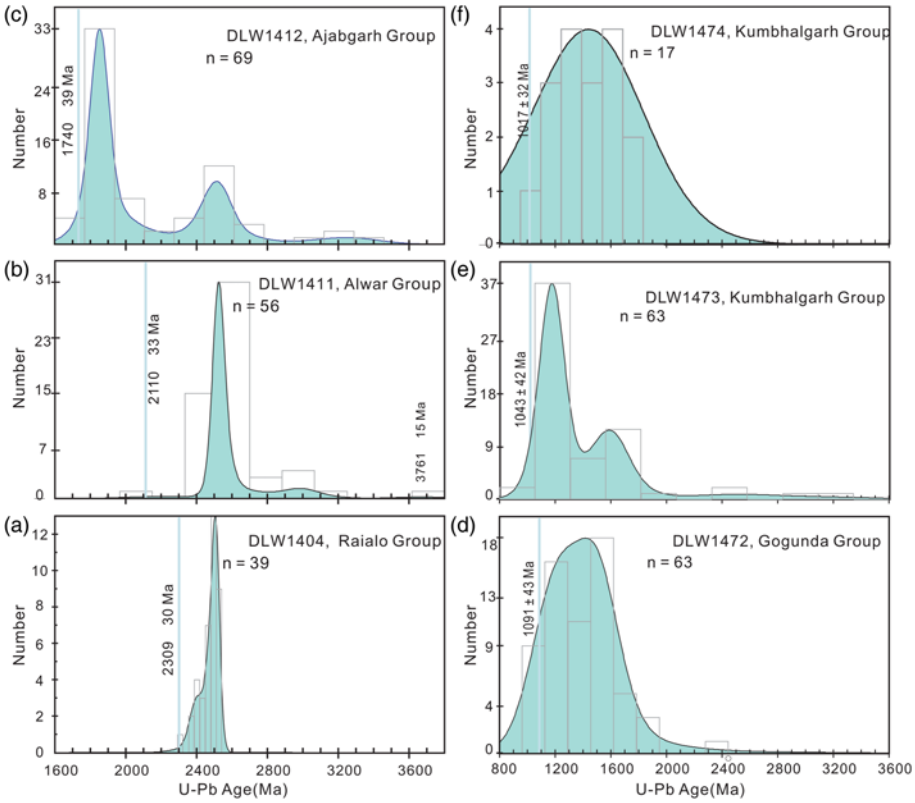

Fig. 7. Age histograms of $^{207}Pb/^{206}Pb$ ages plotted with superimposed kernel density estimates (KDEs) using DensityPlotter (Vermeesch 2012). The vertical bars mark the maximum depositional ages, which are estimated based on $^{207}Pb/^{206}Pb$ ages of the youngest age or weighted mean age of the youngest two zircons. Only U–Pb ages with concordance between 90 and 110% are used for the plotting.

47 (1106 ± 27 Ma), but different from other slightly older zircon grains (e.g. 1115 ± 27 Ma, Fig. 4d). Moreover, spots 60 and 47 have similar U contents (1292 and 1296 ppm) and Th/U ratios (0.82 and 0.73). Thus, the weighted mean age (1091 ± 43 Ma, 2σ) of spots 60 and 47 is considered as the maximum depositional age of the Gogunda sandstone.

The oldest zircon in this sample has a $^{207}Pb/^{206}Pb$ age of 2447 ± 37 Ma and an $\varepsilon_{Hf(t)}$ value of −7.5, similar to the Hf isotopic composition of late Archaean to early Palaeoproterozoic zircon grains from the northeastern segment of the Delhi Supergroup (Fig. 8a). Fifteen zircon grains within the age bracket of 1598 and 1273 Ma have positive $\varepsilon_{Hf(t)}$ values (+5.3 to +1.8), whereas the remaining late Mesoproterozoic zircons (1256 – 1055 Ma) show highly variable $\varepsilon_{Hf(t)}$ values (+2.9 to −10.0) (Fig. 8a). A single 1656 Ma zircon has the highest $\varepsilon_{Hf(t)}$ value of +12.5, close to the value of depleted mantle, within error.

Quartzite from the Kumbhalgarh Group, sample DLW1473

Kumbhalgarh Group quartzite sample DLW1473 was collected west of Udaipur. Zircons from this sample are variably rounded with the majority showing oscillatory zoning, typical of a magmatic origin (Fig. 4e). All the analyses yield concordant U–Pb ages and most of them have $^{207}Pb/^{206}Pb$ ages ranging from 1828 ± 38 to 1043 ± 32 Ma, defining two major clusters (1828 – 1409 and 1283 – 1043 Ma). The youngest two zircon grains, with $^{207}Pb/^{206}Pb$ ages of 1043 ± 32 and 1051 ± 28 Ma, show well-preserved oscillatory zoning and rounded shape, distinct from the dark and ambiguous internal structure of slightly older grains (1081 ± 30 and 1094 ± 30 Ma, Fig. 4e). Furthermore, the two youngest zircons have U concentrations (671 – 432 ppm) lower than but Th/U ratio (0.9 – 0.4) higher than the values (2225 – 1140 ppm, 0.37 – 0.06) of slightly older zircon grains. Thus, the weighted mean $^{207}Pb/^{206}Pb$ age of 1047 ± 42 Ma (2σ) for the youngest two zircon grains is considered as the maximum depositional age of the Kumbhalgarh sandstone. The oldest four zircons have $^{207}Pb/^{206}Pb$ ages from 3227 ± 26 to 2447 ± 40 Ma. All the zircon grains have Th/U ratios between 2.22 and 0.11, except for three grains with ratios less than 0.1 (0.04, 0.07 and 0.06) that have $^{207}Pb/^{206}Pb$ ages of 1256, 1220 and 1094 Ma.

The oldest zircon grain (3227 Ma) has an $\varepsilon_{Hf(t)}$ value of −3.9 and T_{DM2} of 3.8 Ga, whereas a 2861 Ma zircon grain has a depleted mantle-like $\varepsilon_{Hf(t)}$ value of +7.2 with T_{DM2} of 2.8 Ga. Late Palaeoproterozoic to Mesoproterozoic zircons are characterized by variable Hf isotopic compositions with $\varepsilon_{Hf(t)}$ values ranging from +8.9 to −8.0 and T_{DM2} from 2.8 to 1.4 Ga (Fig. 8a).

Calc-siltstone from the Kumbhalgarh Group, sample DLW1474

Sample DLW1474 is a calc-siltstone from the Kumbhalgarh Group. Zircon grains from this sample are relatively small (*c.* 50 μm in length) and show dark oscillatory zoned cores and light luminescent rims (Fig. 4f). The cores of these grains have Th/U ratios from 1.24 to 0.11. Ninety-five per cent of the analyses are concordant with $^{207}Pb/^{206}Pb$ ages ranging from 1794 ± 26 to 1017 ± 32 Ma and form a major peak at *c.* 1.66 Ga (Fig. 7f). The youngest zircon grain shows rounded morphology, different from the angular shape of slightly older grains with uniform internal structures (Fig. 4f), indicating different sources for these zircons. Therefore, the youngest $^{207}Pb/^{206}Pb$ age of 1017 ± 32 Ma is considered to constrain the maximum depositional age of the Kumbhalgarh calc-siltstone. Because of their small size, zircons from this sample were not considered for *in situ* Lu–Hf isotopic analyses.

Discussion

Archaean basement and existence of an Eoarchaean crust

The oldest zircon, with a U–Pb age of 3671 ± 15 Ma, comes from the Alwar Group quartzite sample DLW1411. This sample also contains 2.62 – 2.48 Ga detritus that corresponds to the 2.60 – 2.45 Ga Berach and Ahar River granites of the Banded Gneiss Complex (Wiedenbeck & Goswami 1994; Roy & Kröner

1996). In addition, 3.02, 2.81 and 2.71 Ga detrital zircons in this sample correlate well with a Banded Gneiss Complex source, such as the 2985 ± 49 Ma granite to the north of Jaipur (zircon LA-ICP-MS age; this study), 2828 ± 46 Ma Untala Granite (Sm–Nd whole-rock isochron age) (Gopalan *et al.* 1990), and 2.67 – 2.66 Ga trondhjemites and granitoids to the east and south of Udaipur (zircon evaporation age) (Roy & Kröner 1996). The 2985 Ma granite is also the first report of Archaean age basement from the northern part of the Aravalli mountain region, further confirming a much wider areal distribution for the Archaean basement rocks (Banded Gneiss Complex). The youngest detrital zircon, with a U–Pb age of 2110 ± 33 Ma from sample DLW1411, matches the 2075 – 2150 Ma Pb/Pb age for galena, syngenetically developed within the basal Aravalli mafic volcanic rocks (Deb & Thorpe 2004). Moreover, the oldest zircon grain (3671 Ma) has subhedral morphology with excellent preservation of internal oscillatory zoning (Fig. 4b), implying weak abrasion during a probably short distance of transportation. Taking all the above evidence into consideration, the sedimentary detritus for sample DLW1411 was potentially sourced from the hinterland of NW India and could be representative of the exposed Archaean crust during Delhi sedimentation.

Eoarchaean crustal remnants from Peninsular India are rare and the oldest dated rock so far is the 3585 ± 10 Ma granite from the Bastar craton (Rajesh *et al.* 2009). Detrital zircon with a U–Pb age as old as 3627 ± 39 Ma was reported from the Older Metamorphic Group of the Singhbhum Craton in eastern India (Mishra *et al.* 1999). The gneissic rocks of the Banded Gneiss Complex from the Aravalli region have been dated at 3300, 2900 and 2600 – 2500 Ma (Roy & Kröner 1996) and the oldest detrital zircon, with an age of 3491 ± 7 Ma, comes from the Delwara Formation, the basal segment of the Aravalli Supergroup (McKenzie *et al.* 2013). There are no rocks dated as Eoarchaean or earlier, but Hf isotopes of zircons suggest that formation of Hadean and Eoarchaean crust occurred extensively in the South India Block (Santosh *et al.* 2016). Consequently, the 3671 ± 15 Ma zircon identified in this study is the first Eoarchaean age in NW India and suggests that old crust is present within Peninsular India.

Correlation between the North and South Delhi Supergroup domains

Stratigraphic correlation of rock units across the Delhi Basin is contentious, especially for the depositional age of the North and South Delhi supergroups (Roy & Jakhar 2002; Meert *et al.* 2010; Meert & Pandit 2015). Based on detailed mapping of sedimentary features, Sengupta (1984) concluded that the northern Delhi Supergroup is younger than the inferred correlative strata in the southwestern basin (Sengupta 1984), whereas some other studies suggested an older age for the supergroup (Sinha-Roy 1984; Deb & Thorpe 2004; McKenzie *et al.* 2011). Detrital zircon U–Pb age data underline a predominant Palaeoproterozoic source for detritus from northern supergroup units, and limit the maximum depositional age to *c.* 1720 Ma for the uppermost Ajabgarh Group (Fig. 7a). In contrast, widespread Mesoproterozoic detritus in the South Delhi sedimentary units constrains the initial sedimentation of these units to younger than 1055 Ma (Fig. 7d). Diverse age signatures of provenance for the northeastern and southwestern segments of the Delhi Supergroup preclude any temporal correlation between the two domains (Fig. 3). They most probably have distinct depositional ages and represent either discrete sub-basins or even separate basins.

Episodic reworking and growth of continental crust

The oldest zircon grain has an $\varepsilon_{Hf(t)}$ value (+0.1) lower than that of depleted mantle, hinting at either reworking of recently generated crust or mixing between older continental crust derived melt and mantle-derived melts at 3.67 Ga (Fig. 8a). A wide variation of $\varepsilon_{Hf(t)}$ values for 3.28 – 2.99 and 2.58 – 2.34 Ga zircons implies that both generation of juvenile crust and reworking of older crust occurred during these time intervals. Crustal involvement, not younger than 3.65 Ga, in the reworking process is evidenced by the hafnium model ages (Fig. 8a), synchronous with the 3.67 Ga oldest zircon. This demonstrates the addition of juvenile crust at 3.67 Ga and the hafnium model age of 3.9 Ga represents the maximum estimation of crustal growth within NW India.

Wide $\varepsilon_{Hf(t)}$ variation (+2.7 to −3.9) for 3.28 – 2.99 Ga zircon populations (Fig. 8) implies values between depleted mantle and 3.65 Ga juvenile crust. These observed values and variations could be explained by either reworking of a pre-existing heterogeneous crust or reworking of homogeneous older crust with varying levels of mantle input. Hafnium model ages (T_{DM2}) for these zircons range from 3.6 to 3.2 Ga, with one older age of 3.8 Ga, older than the maximum age of 3.28 Ga obtained for the Banded Gneiss Complex (Wiedenbeck & Goswami 1994). Moreover, only a few 3.59 – 3.25 Ga detrital or xenocrystic zircon grains have been identified in NW India, suggesting limited magmatic activity during this time period. Consequently, the varied $\varepsilon_{Hf(t)}$ values for the 3.28 – 2.99 Ga zircons were possibly generated by reworking of older continental components (not younger than 3.65 Ga) with varying levels of mantle input during the Mesoarchaean (Fig. 8a).

Depleted mantle-like $\varepsilon_{Hf(t)}$ values (+7.2 to +5.6) and T_{DM2} of 2.9 – 2.8 Ga for the 2.86 – 2.71 Ga zircons point toward a depleted mantle source at 2.86 – 2.71 Ga (Fig. 8a). Furthermore, zircons with the lowest $\varepsilon_{Hf(2.11-1.63\ Ga)}$ value correspond to the hafnium model ages of 2.9 – 2.7 Ga (Fig. 8a) and represent the age of old continental crust that was reworking at that time (Fig. 8a). Thus, significant continental crustal growth probably occurred at 2.86 – 2.71 Ga. Figure 8a also hints that new crust formation ceased after 2.71 Ga and that reworking of pre-existing heterogeneous crust was the predominant process during the extensive 2.66 – 2.34 Ga magmatism with mostly subchondritic $\varepsilon_{Hf(t)}$ of zircons; for example, the granitoids of the southern Banded Gneiss Complex (Meert & Pandit 2015). Five zircon grains among this population with positive $\varepsilon_{Hf(t)}$ values of +5.1 to +3.9 have hafnium model ages of 2.8 – 2.6 Ga, indicating reworking of young 'juvenile' crust derived from the depleted mantle between 2.86 and 2.71 Ga, as discussed above. The lowest $\varepsilon_{Hf(2.66-2.34\ Ga)}$ value of −12.1 corresponds to T_{DM2} of 3.6 Ga, largely consistent with an old 'juvenile' crust derived from the depleted mantle at 3.65 Ga as discussed above (Fig. 8a).

As shown in Figure 8a, a large variation in $\varepsilon_{Hf(t)}$ values for Palaeoproterozoic zircons indicates that not only was a substantial volume of older crust reworked but also juvenile crust was formed during these magmatic events. A 1.66 Ga zircon grain has the highest $\varepsilon_{Hf(t)}$ value of +12.1 and hafnium model age identical to its U–Pb age, within error, demonstrating addition of juvenile crust derived from depleted mantle. It is noteworthy that all 2.11 – 2.01 and 1.60 – 1.37 Ga zircons have super-chondritic $\varepsilon_{Hf(t)}$ values (+7.8 to +0.2) (Fig. 8a), indicating emplacement of depleted mantle-derived magma that was rapidly reworked or contaminated by older crust.

A distinct 1.31 – 1.04 Ga thermal event is clearly demonstrated in the histogram of the southern Delhi Supergroup detrital zircon ages (Fig. 8b). The Hf isotopic data ($\varepsilon_{Hf(t)}$ = +9.6 to −10.0) indicate that the host rocks of these zircons were largely developed through reworking of heterogeneous older crustal components or through reworking of homogeneous older crust with varying levels of mantle input (Fig. 8a). Most of these zircons have $\varepsilon_{Hf(t)}$ values between +4.8 and −10.0, much lower than the value of depleted mantle (Fig. 8a), indicating that juvenile material from depleted mantle was limited during the 1.31 – 1.04 Ga time interval. On the

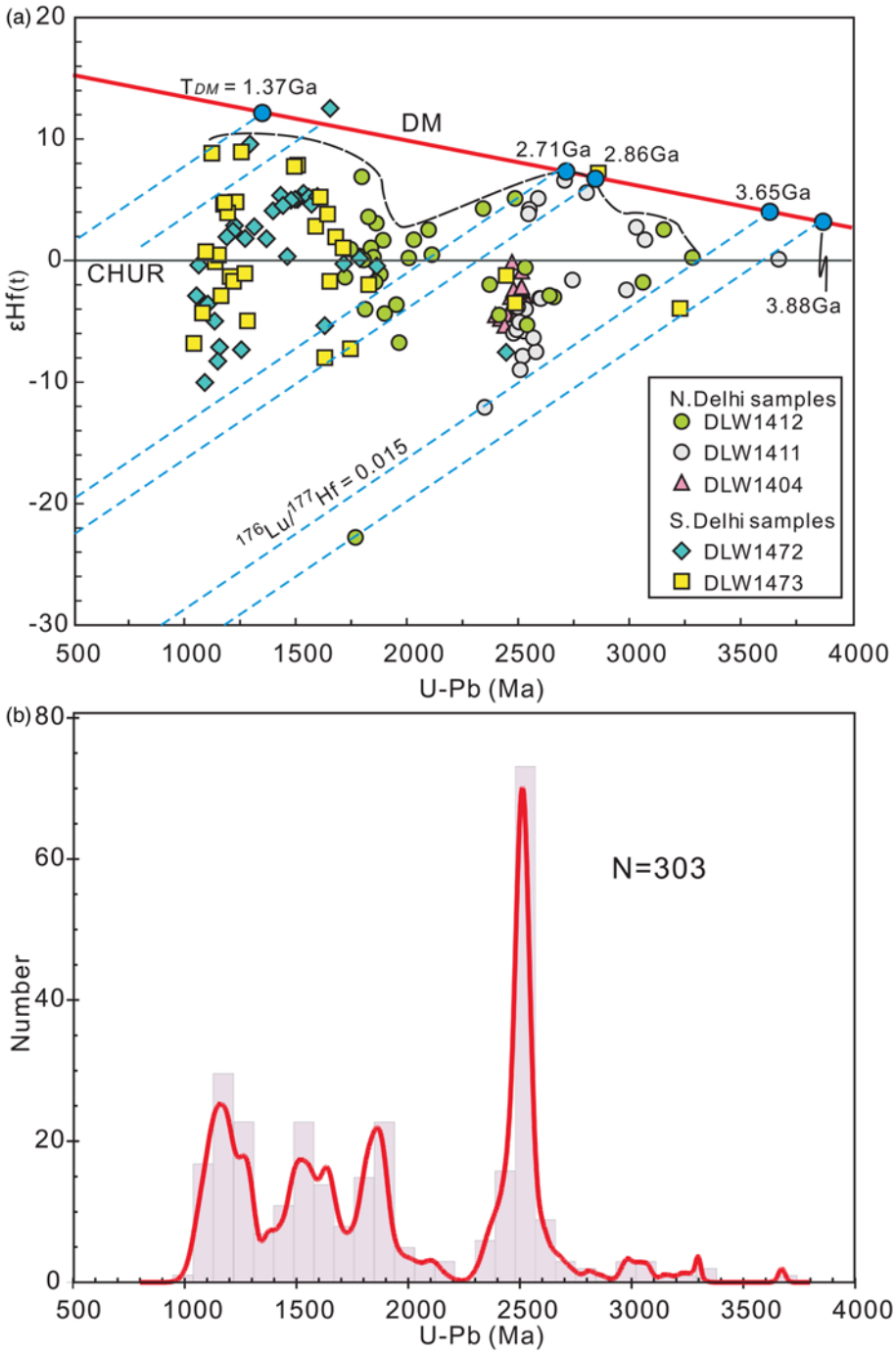

Fig. 8. (**a**) Synopsis of $\varepsilon_{Hf(t)}$ data for detrital zircon grains from the Delhi Supergroup. CHUR, chondritic uniform reservoir; DM, depleted mantle; T_{DM}, hafnium model ages. (**b**) Age histograms of analysed zircon grains from the Delhi Supergroup. Only concordant analyses are used for plotting.

other hand, the 1.31 – 1.04 Ga zircons have $\varepsilon_{Hf(t)}$ values similar to those for evolved crust that were derived from a depleted mantle, between 2.71 and 1.37 Ga (Fig. 8a). Highly variable but evenly distributed $\varepsilon_{Hf(t)}$ values suggest significant contributions from both older (2.71 Ga) and younger (1.37 Ga) continental crust during the generation of the zircon hosting magma (Fig. 8a).

Possible linkage between India and Cathaysia Block during supercontinent cycles

The major peaks in the detrital zircon age distributions of the Delhi Supergroup correlate well with periods of supercontinent assembly (Fig. 9a), reflecting involvement of the northwestern Indian block in the supercontinent cycles from Nuna to Rodinia. The western margin of the Indian shield was argued by Zhao *et al.* (2002) to have been adjacent to the northern margin of the North China Craton at *c.* 1.8 Ga, whereas the Trans-North China Orogen represents a block contiguous to the Central Indian Tectonic Zone, the suture between the Northern and Southern Indian blocks. Three episodes of granulite-facies metamorphism have been recognized between 1.66 and 1.54 Ga in the Central Indian Tectonic Zone (Bhowmik *et al.* 2014), considerably younger than the *c.* 1.85 Ga Trans-North China Orogen (Zhao *et al.* 2002). Moreover, the detrital zircon age distributions of coeval rift-related sequences from the two continents show distinct patterns (e.g. *c.* 1.95 v. *c.* 1.85 Ga peak) (Fig.10), arguing against any connection between them. Alternatively, the eastern margin of the Indian shield was proposed to be connected to the southern North China Craton (Hou *et al.* 2008), whereas the southern margin of the North China Craton was considered to be a continental margin arc and could not be connected to any other continents (Zhao *et al.* 2011*a*).

NW India has also been tentatively placed close to the southwestern Yangtze Block on the basis of similar style of copper mineralization; for example, the Khetri copper belt in NW

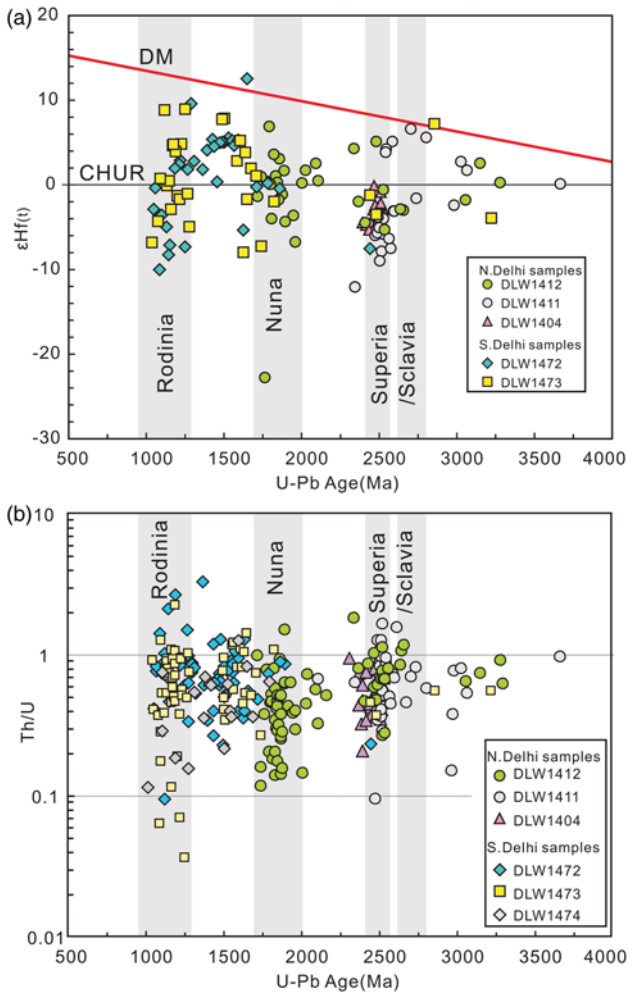

Fig. 9. (**a**) Synopsis of $\varepsilon_{Hf(t)}$ data for detrital zircon grains from the Delhi Supergroup showing the variation of $\varepsilon_{Hf(t)}$ values corresponding to supercontinent cycles; (**b**) variation of Th/U ratios is also consistent with the supercontinent process; for example, assembly of a supercontinent is associated with large variation in Th/U ratios. Only concordant analyses are used for plotting.

India and the Dahongshan deposits in SW Yangtze (Zhou *et al.* 2014). Nonetheless, a 1.97 – 1.95 Ga metamorphic event linking the Yangtze Block with NW Laurentia in the Nuna supercontinent predates the formation of the Central Indian Tectonic Zone (1.66 – 1.54 Ga) and the Aravalli accretionary orogenesis (*c.* 1.84 – 1.82 Ga) (Fig. 9) (Bhowmik & Dasgupta 2012; Bhowmik *et al.* 2014; Wang *et al.* 2016), inconsistent with the Yangtze–India connection. Two episodes (*c.* 1.71 and 1.68 – 1.66 Ga) of within-plate magmatism in the southwestern Yangtze Block show bimodal assemblages (Chen *et al.* 2013), different from the *c.* 1.72 Ga felsic-dominated magmatism and granulite-facies metamorphism in the Aravalli–Delhi Fold Belt (Biju-Sekhar *et al.* 2003; Buick *et al.* 2006, 2010; Bhowmik & Dasgupta 2012). Moreover, detrital zircon age patterns of *c.* 1.74 – 1.50 Ga sedimentary rocks in the SW Yangtze Block show distinct peaks at *c.* 2.85, *c.* 2.76 and *c.* 2.31 Ga, which are distinct from those for the Delhi Supergroup (Fig. 10). These observations argue against any possible linkage between NW India and the SW Yangtze Block within a Nuna reconstruction.

A close link between the Lesser Himalaya and the eastern Cathaysia Block is proposed on the basis of similarity in geochemical signatures of 1.90 – 1.84 Ga felsic igneous rocks and U–Pb–Hf isotope compositions of detrital zircons from the two regions (Yu *et al.* 2012, and references therein). The 1.89 – 1.85 Ga orogeny in the eastern Cathaysia Block is believed to be similar to

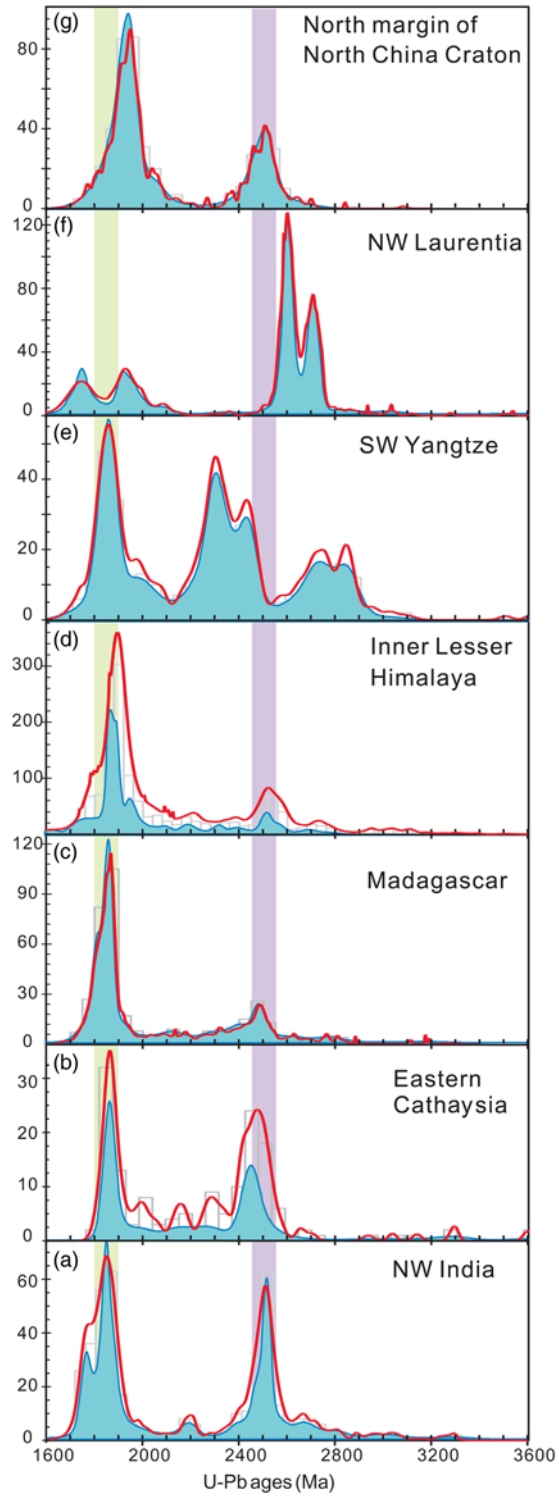

Fig. 10. U–Pb age spectra of zircons from metasedimentary rocks of (**a**) northern Aravalli orogen (data source: Kaur *et al.* 2011; this study), (**b**) eastern Cathaysia Block, South China (data source: Yu *et al.* 2012), (**c**) Madagascar (data source: Bauer *et al.* 2011; De Waele *et al.* 2011), (**d**) inner Lesser Himalaya (data source: Parrish & Hodges 1996; Richards *et al.* 2005; McQuarrie *et al.* 2008; Long *et al.* 2011; Martin *et al.* 2011; McKenzie *et al.* 2011), (**e**) southwestern Yangtze Block (data source: Zhao *et al.* 2010; Wang *et al.* 2012; Wang & Zhou 2014), (**f**) northwestern Laurentia (data source: Rainbird & Davis 2007), (**g**) northern margin of North China Craton (data source: Ma *et al.* 2014; Zhong *et al.* 2015). The vertical reference bars are at 1.85 and 2.5 Ga. Only those rocks that show a late Palaeoproterozoic (1.9 – 1.6 Ga) maximum age of deposition and the zircons with 90 – 110% concordance level were considered. The shaded areas under the curves refer to kernel density estimate plots (Vermeesch 2012).

that in the Lesser Himalaya (Yu *et al.* 2012). However, possible connections between the Lesser Himalaya and the Aravalli orogen are obscured by the alluvium in the intervening Indo-Gangetic plains and Eocene shortening of the northern India margin. Recent multi-fold deep seismic reflection profiling has shown *c.* 1.85 Ga basement rocks below the Sub-Himalayan region and the Indo-Gangetic plains, similar to those exposed in the Aravalli Orogen (Rajendra Prasad *et al.* 2011). In addition, strikingly similar detrital zircon age distributions were observed for Himalayan and age-equivalent successions of the Indian shield, suggesting a close proximity between the two regions during late Palaeoproterozoic to Early Cambrian times (McKenzie *et al.* 2011). This connection confirms the linkage between North India, the Lesser Himalaya and the eastern Cathaysia Block, which is reinforced by the similarity in detrital zircon age distribution, during the assembly of Nuna (Figs 10 and 11a). In addition, the inferred widely distributed *c.* 2.5 Ga basement with 3.7 – 3.6 and 3.3 – 3.0 Ga crustal remnants in the Cathaysia Block recorded by detrital or inherited zircons (Yu *et al.* 2008) correlates well with the dated 3.3 – 2.9 Ga gneisses and 2.60 – 2.45 Ga granitoids within the Banded Gneiss Complex (Wiedenbeck & Goswami 1994; Roy & Kröner 1996). On the other hand, western India and northern Madagascar may have been linked since the assembly of Nuna (*c.* 1.85 Ga) based on the remarkably similar age distribution of detrital zircons from contemporary strata in the two regions (Figs 10 and 11a).

The spatial linkage between northern India and the Cathaysia Block of South China was probably sustained until the break-up of Pangaea (Cawood *et al.* 2013*b*). The position of the South China Block in Rodinia is disputed (Zheng 2004; Li *et al.* 2008; Yu *et al.* 2008; Zhao *et al.* 2011*b*; Wang & Zhou 2012; Cawood *et al.* 2013*b*). However, a synthesis of available geological, geochemical, geochronological, palaeomagnetic and faunal data demonstrates that the South China Block has maintained a position off western Australia and northeastern India along the periphery of both the Rodinia and Gondwana supercontinents (Fig. 11). Cawood *et al.* (2013*b*) suggested that the South China Block was adjacent to northeastern India since at least the beginning of the Neoproterozoic and represented a preserved fragment of greater India lithosphere until rifting off during early break-up of Pangaea. This linkage between India and the eastern Cathaysia Block of South China could probably be traced back to the assembly of the Nuna supercontinent (Fig. 11). The Yangtze Block was an exotic terrane accreted to the eastern Cathaysia–northern India united continent between 1000 and 820 Ma through a succession of suprasubduction-zone arc–back-arc systems that developed in the southeastern Yangtze and northwestern Cathaysia blocks (Cawood *et al.* 2013*b*, and references therein). From *c.* 870 to 706 Ma subduction-related igneous rocks developed along the northern to western margins of the Yangtze Block (Zhou *et al.* 2006; Zhao & Zhou 2007), and these correlate well, in terms of age, rock assemblages and geochemistry, with volcanic and plutonic rocks in northern and north–central Madagascar, northwestern India and the Seychelles (Torsvik *et al.* 2001; Tucker *et al.* 2001; Ashwal *et al.* 2013), defining an active continental margin along the periphery of the Rodinia supercontinent (Fig. 9), although various models have been proposed regarding the petrogenesis and tectonic affinity of the Neoproterozoic igneous rocks in South China (Li *et al.* 1999, 2003; Wang *et al.* 2006; Zheng *et al.* 2008). Amalgamation of the Yangtze and Cathaysia blocks formed the South China Block, which remained juxtaposed to India until its separation from Pangaea in the late Palaeozoic (Fig. 11) (Metcalfe 2011; Cawood *et al.* 2013*b*).

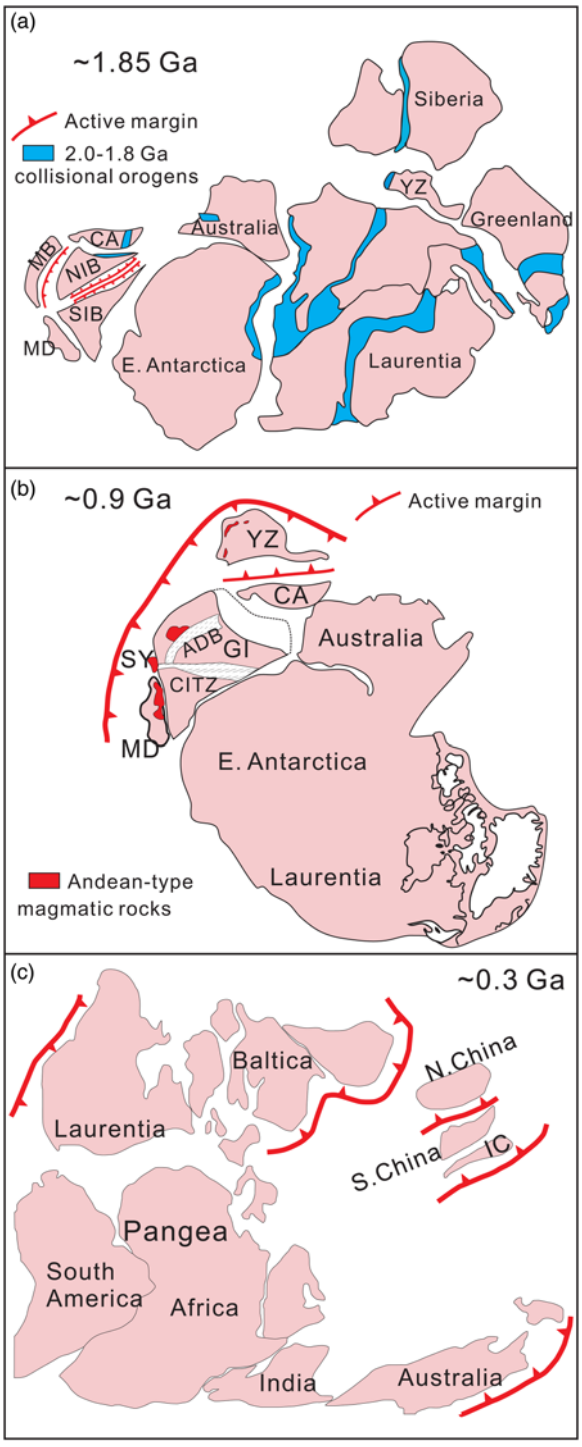

Fig. 11. Schematic palaeogeographical reconstructions showing position of Indian shield and its relationship with the South China Block (including the Yangtze and Cathaysia blocks). (**a**) Nuna assembly at *c.* 1.85 Ga (adapted from Zhao *et al.* 2002; Yu *et al.* 2012; Wang *et al.* 2016). The active margin in the western and southern margins of the Northern Indian Block is adapted from Bhowmilk *et al.* (2012). (**b**) Rodinia assembly at *c.* 900 Ma (adapted from Cawood *et al.* 2013*b*). (**c**) Pangaea assembly at *c.* 300 Ma (adapted from Metcalfe 2011; Cawood *et al.* 2013*b*). YZ, Yangtze Block; CA, Cathaysia Block; MB, Marwar Block; NIB, Northern Indian Block; SIB, Southern Indian Block; MD, Madagascar; SY, Seychelles; GI, Greater India; ADB, Aravalli–Delhi Fold Belt; CITZ, Central Indian Tectonic Zone; IC, Indo-China Block.

Crustal growth, reworking and supercontinent cycles

Periodic assembly and dispersal of continental blocks constitutes the supercontinent cycle, which is associated with variable growth rate of continental crust throughout the Earth's history (Hawkesworth *et al.* 2010; Roberts 2012; Cawood *et al.* 2013*a*; Spencer *et al.* 2015). Wide variations in Th/U ratios for zircons during the assembly of supercontinents (Fig. 9b) reflect their

magmatic (Th/U > 0.1) and metamorphic (Th/U < 0.1) origin and association with continental assembly. Three clusters, wherein $\varepsilon_{Hf(t)}$ values of the Delhi zircons extend vertically into both positive and negative space (Fig. 9a), suggest involvement of both relatively juvenile and reworked continental crust. A small fraction (*c.* 9%) of 2590 – 2343 Ma zircons have positive $\varepsilon_{Hf(t)}$, indicating that the highest capture rate of reworked crust was during the formation of the Superia continent, whereas the assembly of Nuna and Rodinia was associated with larger amounts of juvenile crust as revealed by higher fractions (*c.* 48 and 39%) with positive $\varepsilon_{Hf(t)}$ values (Fig. 9a). Capture of more juvenile crust during late Palaeoproterozoic to Mesoproterozoic supercontinent assembly is thought to be consistent with the widespread thick and strong lithosphere under giant orogens (Condie *et al.* 2011). In contrast, nearly all zircons with ages corresponding to convergent and divergent settings during supercontinent cycles have depleted mantle-like positive $\varepsilon_{Hf(t)}$ values (Fig. 9a), indicating either a better preservation of juvenile crust compared with reworked crust or a dominant contribution of juvenile crust during the period between break-up and assembly of supercontinents. A changing balance of continental addition v. loss during supercontinent cycles is considered a major reason for the growth of continental crust (Roberts 2012; Cawood *et al.* 2013*a*). This observation is consistent with the inference that both convergent and extensional settings are locales of net growth of continental crust, whereas a collisional setting is characterized by greater removal than juvenile addition of crust (Cawood *et al.* 2013*a*; Spencer *et al.* 2015). Nonetheless, the small fraction of such zircons is generally taken as evidence that there was only minor juvenile continental crustal addition during rifting of supercontinents (Condie *et al.* 2011). An observed punctuated rock record is biased by the formation of supercontinents (Hawkesworth *et al.* 2009, 2010) and represents integration of volumes of magma generated during assembly and break-up of a supercontinent and their preservation potential within each of these phases (Hawkesworth *et al.* 2009; Cawood *et al.* 2013*a*; Spencer *et al.* 2015). The preservation potential of rocks in convergent and extensional settings is less than during phases of continental amalgamation, resulting in observed peaks, which may not be related to underlying variation in the rate of crust generation (Hawkesworth *et al.* 2009; Cawood *et al.* 2013*a*; Spencer *et al.* 2015). Therefore, zircons for which ages correspond to the subduction and break-up during supercontinent cycles are not likely to be as well preserved (e.g. Hawkesworth *et al.* 2009; Cawood *et al.* 2013*a*; Spencer *et al.* 2015).

Concluding remarks

The *in situ* U–Pb and Hf isotopic data for detrital zircons from the Delhi Supergroup have identified wide variations in the T_{DM2} and $\varepsilon_{Hf(t)}$ values for 3.28 – 2.99 and 2.58 – 2.34 Ga zircons, suggesting both generation of juvenile crust and reworking of older crust at these time intervals in NW India. Juvenile crust derived from depleted mantle source was added at 2.86 – 2.71 Ga, whereas crustal reworking of pre-existing heterogeneous crust was the predominant process for the extensive 2.66 – 2.34 Ga magmatism (mostly subchondritic $\varepsilon_{Hf(t)}$) in NW India. Large variation in $\varepsilon_{Hf(t)}$ values for Palaeo- to Mesoproterozoic zircons indicates that reworking of older crust and addition of juvenile crust occurred at 2.11 – 2.01 Ga and 1.60 – 1.37 Ga, respectively. The oldest zircon, with an age of 3671 ± 15 Ma, reflects the possible existence of a Eoarchaean crust in NW India, with a crustal growth event as early as at 3.9 Ga. Consistency between detrital age peaks and supercontinent cycles reflects involvement of the Indian shield in Nuna to Rodinia supercontinent cycles. Zircon Hf isotopes suggest that assembly of supercontinents was associated with both juvenile crust formation and remelting of the ancient continental crust, whereas pre-collision and break-up of the supercontinent corresponds to predominant juvenile crustal addition. The northern Indian shield was most probably connected to the Cathaysia Block of South China during assembly of Nuna and these two crustal fragments remained together until the break-up of Pangaea.

Acknowledgements We would like to thank Z. Hu for (MC)-LA-ICP-MS analyses. V. K. Meena is thanked for his generous help during fieldwork. Constructive comments from two anonymous reviewers and Editor C. Clark helped to significantly improve the paper.

Funding This study was supported by the National Natural Science Foundation of China (NSFC 41572170), 'Thousand Youth Talents Plan' grants to W.W. and W.-T.C. and MOST Special Fund from the State Key Laboratory of Geological Processes and Mineral Resources (MSFGPMR11 and 01-1) from China University of Geosciences (Wuhan). P.A.C. acknowledges support from Australian Research Council grant FL160100168.

Scientific editing by Chris Clark

References

Amelin, Y., Lee, D.-C., Halliday, A.N. & Pidgeon, R.T. 1999. Nature of the Earth's earliest crust from hafnium isotopes in single detrital zircons. *Nature*, **399**, 252–255.

Ashwal, L., Solanki, A., Pandit, M., Corfu, F., Hendriks, B., Burke, K. & Torsvik, T. 2013. Geochronology and geochemistry of Neoproterozoic Mt. Abu granitoids, NW India: Regional correlation and implications for Rodinia paleogeography. *Precambrian Research*, **236**, 265–281.

Bauer, W., Walsh, G.J. *et al.* 2011. Cover sequences at the northern margin of the Antongil Craton, NE Madagascar. *Precambrian Research*, **189**, 292–312.

Bhowmik, S.K. & Dasgupta, S. 2012. Tectonothermal evolution of the Banded Gneissic Complex in central Rajasthan, NW India: Present status and correlation. *Journal of Asian Earth Sciences*, **49**, 339–348.

Bhowmik, S.K., Wilde, S.A., Bhandari, A. & Basu Sarbadhikari, A. 2014. Zoned monazite and zircon as monitors for the thermal history of granulite terranes: an example from the Central Indian Tectonic Zone. *Journal of Petrology*, **55**, 585–621.

Biju-Sekhar, S., Yokoyama, K., Pandit, M.K., Okudaira, T., Yoshida, M. & Santosh, M. 2003. Late Palaeoproterozoic magmatism in Delhi Fold Belt, NW India and its implication: evidence from EPMA chemical ages of zircons. *Journal of Asian Earth Sciences*, **22**, 189–207.

Blichert-Toft, J. & Albarède, F. 1997. The Lu–Hf isotope geochemistry of chondrites and the evolution of the mantle–crust system. *Earth and Planetary Science Letters*, **148**, 243–258.

Buick, I.S., Allen, C., Pandit, M., Rubatto, D. & Hermann, J. 2006. The Proterozoic magmatic and metamorphic history of the Banded Gneiss Complex, central Rajasthan, India: LA-ICP-MS U–Pb zircon constraints. *Precambrian Research*, **151**, 119–142.

Buick, I., Clark, C., Rubatto, D., Hermann, J., Pandit, M. & Hand, M. 2010. Constraints on the Proterozoic evolution of the Aravalli–Delhi Orogenic belt (NW India) from monazite geochronology and mineral trace element geochemistry. *Lithos*, **120**, 511–528.

Cawood, P.A., Nemchin, A.A., Strachan, R., Prave, T. & Krabbendam, M. 2007. Sedimentary basin and detrital zircon record along East Laurentia and Baltica during assembly and breakup of Rodinia. *Journal of the Geological Society, London*, **164**, 257–275.

Cawood, P.A., Hawkesworth, C.J. & Dhuime, B. 2012. Detrital zircon record and tectonic setting. *Geology*, **40**, 875–878.

Cawood, P.A., Hawkesworth, C. & Dhuime, B. 2013*a*. The continental record and the generation of continental crust. *Geological Society of America Bulletin*, **125**, 14–32.

Cawood, P.A., Wang, Y., Xu, Y. & Zhao, G. 2013*b*. Locating South China in Rodinia and Gondwana: A fragment of greater India lithosphere? *Geology*, **41**, 903–906.

Chen, W.T., Zhou, M.-F. & Zhao, X.-F. 2013. Late Palaeoproterozoic sedimentary and mafic rocks in the Hekou area, SW China: Implication for the reconstruction of the Yangtze Block in Columbia. *Precambrian Research*, **231**, 61–77.

Chu, N., Taylor, R. *et al.* 2002. Hf isotope ratio analysis using multi-collector inductively coupled plasma mass spectrometry: an evaluation of isobaric interference corrections. *Journal of Analytical Atomic Spectrometry*, **17**, 1567–1574.

Condie, K.C., Bickford, M.E., Aster, R.C., Belousova, E. & Scholl, D.W. 2011. Episodic zircon ages, Hf isotopic composition, and the preservation rate of continental crust. *Geological Society of America Bulletin*, **123**, 951–957.

Deb, M. & Thorpe, R. 2004. Geochronological constraints in the Precambrian geology of Rajasthan and their metallogenic implications. *In*: Deb, M. & Goodfellow, W.D. (eds) *Sediment-Hosted Lead-Zinc Sulphide Deposits*. Narosa, New Delhi, 246–263.

De Waele, B., Thomas, R.J. *et al.* 2011. Provenance and tectonic significance of the Palaeoproterozoic metasedimentary successions of central and northern Madagascar. *Precambrian Research*, **189**, 18–42.

Dhuime, B., Hawkesworth, C.J., Cawood, P.A. & Storey, C.D. 2012. A change in the geodynamics of continental growth 3 billion years ago. *Science*, **335**, 1334–1336.

Gopalan, K., Macdougall, J.D., Roy, A.B. & Murali, A.V. 1990. Sm–Nd evidence for 3.3 Ga old rocks in Rajasthan, northwestern India. *Precambrian Research*, **48**, 287–297.

Griffin, W.L., Pearson, N.J., Belousova, E., Jackson, S.E., Van Achterbergh, E., O'Reilly, S.Y. & Shee, S.R. 2000. The Hf isotope composition of cratonic mantle: LAM-MC-ICPMS analysis of zircon megacrysts in kimberlites. *Geochimica et Cosmochimica Acta*, **64**, 133–148.

Gupta, S. 1997. *The Precambrian geology of the Aravalli region, southern Rajasthan and northeastern Gujarat*. Geological Survey of India, Hyderabad.

Gupta, S.N., Arora, Y.K., Mathur, R.K., Iqbalduddin Prasad, B., Sahai, T.N. & Sharma, S.B. 1980. *Lithostratigraphic Map of Aravalli Region, Southern Rajasthan and Northeastern Gujarat*. Geological Survey of India, Hyderabad.

Harrison, T.M. 2009. The Hadean crust: evidence from >4 Ga zircons. *Annual Review of Earth and Planetary Sciences*, **37**, 479–505.

Hawkesworth, C., Cawood, P., Kemp, T., Storey, C. & Dhuime, B. 2009. Geochemistry: A matter of preservation. *Science*, **323**, 49–50.

Hawkesworth, C.J., Dhuime, B., Pietranik, A.B., Cawood, P.A., Kemp, A.I.S. & Storey, C.D. 2010. The generation and evolution of the continental crust. *Journal of the Geological Society, London*, **167**, 229, https://doi.org/10.1144/0016-76492009-072

Heron, A.M. 1953. *Geology of Central Rajputana*. Geological Society of India, Bangalore, Memoirs, **79**.

Horstwood, M.S.A., Košler, J. *et al.* 2016. Community-derived standards for LA-ICP-MS U–(Th–)Pb geochronology – uncertainty propagation, age interpretation and data reporting. *Geostandards and Geoanalytical Research*, **40**, 311–332.

Hou, G., Santosh, M., Qian, X., Lister, G.S. & Li, J. 2008. Configuration of the Late Palaeoproterozoic supercontinent Columbia: Insights from radiating mafic dyke swarms. *Gondwana Research*, **14**, 395–409.

Iizuka, T. & Hirata, T. 2005. Improvements of precision and accuracy in *in situ* Hf isotope microanalysis of zircon using the laser ablation-MC-ICPMS technique. *Chemical Geology*, **220**, 121–137.

Jackson, S., Pearson, N., Griffin, W., & Belousova, E. 2004. The application of laser ablation-inductively coupled plasma-mass spectrometry to in situ U-Pb zircon geochronology. *Chemical Geology*, **211**, 47–69.

Kaur, P., Zeh, A., Chaudhri, N., Gerdes, A. & Okrusch, M. 2011. Archaean to Palaeoproterozoic crustal evolution of the Aravalli mountain range, NW India, and its hinterland: The U–Pb and Hf isotope record of detrital zircon. *Precambrian Research*, **187**, 155–164.

Kaur, P., Zeh, A., Chaudhri, N., Gerdes, A. & Okrusch, M. 2013. Nature of magmatism and sedimentation at a Columbia active margin: Insights from combined U-Pb and Lu-Hf isotope data of detrital zircons from NW India. *Gondwana Research*, **23**, 1040–1052.

Kemp, A.I.S., Wilde, S.A. *et al.* 2010. Hadean crustal evolution revisited: New constraints from Pb–Hf isotope systematics of the Jack Hills zircons. *Earth and Planetary Science Letters*, **296**, 45–56.

Kusiak, M.A., Whitehouse, M.J., Wilde, S.A., Nemchin, A.A. & Clark, C. 2013. Mobilization of radiogenic Pb in zircon revealed by ion imaging: Implications for early Earth geochronology. *Geology*, **41**, 291–294.

Li, X.H., Li, Z.X., Ge, W., Zhou, H., Li, W., Liu, Y. & Wingate, M.T.D. 2003. Neoproterozoic granitoids in South China: crustal melting above a mantle plume at *ca*. 825 Ma? *Precambrian Research*, **122**, 45–83.

Li, Z.X., Li, X.H., Kinny, P.D. & Wang, J. 1999. The breakup of Rodinia: did it start with a mantle plume beneath South China? *Earth and Planetary Science Letters*, **173**, 171–181.

Li, Z.X., Bogdanova, S.V. *et al.* 2008. Assembly, configuration, and break-up history of Rodinia: A synthesis. *Precambrian Research*, **160**, 179–210.

Liu, Y.S., Gao, S., Hu, Z.C., Gao, C., Zong, K. & Wang, D. 2010. Continental and oceanic crust recycling-induced melt–peridotite interactions in the Trans-North China Orogen: U–Pb dating, Hf isotopes and trace elements in zircons from mantle xenoliths. *Journal of Petrology*, **51**, 537–571.

Long, S., McQuarrie, N., Tobgay, T., Rose, C., Gehrels, G. & Grujic, D. 2011. Tectonostratigraphy of the Lesser Himalaya of Bhutan: Implications for the along-strike stratigraphic continuity of the northern Indian margin. *Geological Society of America Bulletin*, **123**, 1406–1426.

Ludwig, K.R. 2003. *User's Manual for Isoplot 3.00, a Geolochronolgical Toolkit for Microsoft Excel*. Berkeley Geochronology Center, Special Publication, **4**, 25–32.

Ma, M.Z., Zhang, Y.X., Xie, H.Q. & Wan, Y.S. 2014. SHRIMP U–Pb dating and LA-ICPMS Hf isotope analysis of detrital zircons from medium- to coarse-grained sandstones of the Bayan Obo Group and Sailinhudong Group and its geological significances. *Acta Petrologica Sinica*, **30**, 2973–2988.

Martin, A.J., Burgy, K.D., Kaufman, A.J. & Gehrels, G.E. 2011. Stratigraphic and tectonic implications of field and isotopic constraints on depositional ages of Proterozoic Lesser Himalayan rocks in central Nepal. *Precambrian Research*, **185**, 1–17.

McKenzie, N.R., Hughes, N.C., Myrow, P.M., Xiao, S. & Sharma, M. 2011. Correlation of Precambrian–Cambrian sedimentary successions across northern India and the utility of isotopic signatures of Himalayan lithotectonic zones. *Earth and Planetary Science Letters*, **312**, 471–483.

McKenzie, N.R., Hughes, N.C., Myrow, P.M., Banerjee, D.M., Deb, M. & Planavsky, N.J. 2013. New age constraints for the Proterozoic Aravalli–Delhi successions of India and their implications. *Precambrian Research*, **238**, 120–128.

McQuarrie, N., Robinson, D., Long, S., Tobgay, T., Grujic, D., Gehrels, G. & Ducea, M. 2008. Preliminary stratigraphic and structural architecture of Bhutan: Implications for the along strike architecture of the Himalayan system. *Earth and Planetary Science Letters*, **272**, 105–117.

Meert, J.G. & Pandit, M.K. 2015. The Archaean and Proterozoic history of Peninsular India: tectonic framework for Precambrian sedimentary basins in India. *In*: *Geological Society, London, Memoirs*, **43**, 29–54, https://doi.org/10.1144/M43.3

Meert, J.G., Pandit, M.K. *et al.* 2010. Precambrian crustal evolution of Peninsular India: A 3.0 billion year odyssey. *Journal of Asian Earth Sciences*, **39**, 483–515.

Metcalfe, I. 2011. Tectonic framework and Phanerozoic evolution of Sundaland. *Gondwana Research*, **19**, 3–21.

Mishra, S., Deomurari, M.P., Wiedenbeck, M., Goswami, J.N., Ray, S. & Saha, A.K. 1999. $^{207}Pb/^{206}Pb$ zircon ages and the evolution of the Singhbhum Craton, eastern India: an ion microprobe study. *Precambrian Research*, **93**, 139–151.

Parrish, R. & Hodges, V. 1996. Isotopic constraints on the age and provenance of the Lesser and Greater Himalayan sequences, Nepalese Himalaya. *Geological Society of America Bulletin*, **108**, 904–911.

Patchett, P.J., Kouvo, O., Hedge, C.E. & Tatsumoto, M. 1981. Evolution of continental crust and mantle heterogeneity: evidence from Hf isotopes. *Contributions to Mineralogy and Petrology*, **78**, 279–297.

Rainbird, R. & Davis, W. 2007. U–Pb detrital zircon geochronology and provenance of the late Paleoproterozoic Dubawnt Supergroup: Linking sedimentation with tectonic reworking of the western Churchill Province, Canada. *Geological Society of America Bulletin*, **119**, 314–328.

Rajendra Prasad, B., Klemperer, S.L., Vijaya Rao, V., Tewari, H.C. & Khare, P. 2011. Crustal structure beneath the Sub-Himalayan fold–thrust belt, Kangra recess, northwest India, from seismic reflection profiling: Implications for Late Palaeoproterozoic orogenesis and modern earthquake hazard. *Earth and Planetary Science Letters*, **308**, 218–228.

Rajesh, H., Mukhopadhyay, J., Beukes, N., Gutzmer, J., Belyanin, G. & Armstrong, R. 2009. Evidence for an early Archaean granite from Bastar craton, India. *Journal of the Geological Society, London*, **166**, 193–196, https://doi.org/10.1144/0016-76492008-089

Reimink, J.R., Chacko, T., Stern, R.A. & Heaman, L.M. 2014. Earth's earliest evolved crust generated in an Iceland-like setting. *Nature Geoscience*, **7**, 529–533.

Reimink, J.R., Davies, J.H.F.L. *et al.* 2016. No evidence for Hadean continental crust within Earth's oldest evolved rock unit. *Nature Geoscience*, **9**, 777–780.

Richards, A., Argles, T., Harris, N., Parrish, R., Ahmad, T., Darbyshire, F. & Draganits, E. 2005. Himalayan architecture constrained by isotopic tracers from clastic sediments. *Earth and Planetary Science Letters*, **236**, 773–796.

Roberts, N.M.W. 2012. Increased loss of continental crust during supercontinent amalgamation. *Gondwana Research*, **21**, 994–1000.

Rogers, J. & Santosh, M. 2002. Configuration of Columbia, a Mesoproterozoic supercontinent. *Gondwana Research*, **5**, 5–22.

Roy, A.B. & Jakhar, S.R. 2002. *Geology of Rajasthan: Precambrian to Recent*. Scientific Publishers (India), Jodhpur.

Roy, A.B. & Kröner, A. 1996. Single zircon evaporation ages constraining the growth of the Archaean Aravalli craton, northwestern Indian shield. *Geological Magazine*, **133**, 333–342.

Santosh, M., Yang, Q.-Y., Shaji, E., Mohan, M.R., Tsunogae, T. & Satyanarayanan, M. 2016. Oldest rocks from Peninsular India: Evidence for Hadean to Neoarchaean crustal evolution. *Gondwana Research*, **29**, 105–135.

Sengupta, S. 1984. A reinterpretation of the stratigraphy of central Rajasthan between Rajosi and Chowdasya, Ajmer District, Rajasthan. India. *Indian Journal of Geology*, **11**, 38–49.

Sinha-Roy, S. 1984. Precambrian crustal interaction in Rajasthan, NW India. *Indian Journal of Earth Sciences*, **11**, 84–91.

Söderlund, U., Patchett, P.J., Vervoort, J.D. & Isachsen, C.E. 2004. The ^{176}Lu decay constant determined by Lu–Hf and U–Pb isotope systematics of Precambrian mafic intrusions. *Earth and Planetary Science Letters*, **219**, 311–324.

Spencer, C.J., Cawood, P.A., Hawkesworth, C.J., Prave, A.R., Roberts, N.M.W., Horstwood, M.S.A. & Whitehouse, M.J. 2015. Generation and preservation of continental crust in the Grenville Orogeny. *Geoscience Frontiers*, **6**, 357–372.

Spencer, C.J., Kirkland, C.L. & Taylor, R.J.M. 2016. Strategies towards statistically robust interpretations of *in situ* U–Pb zircon geochronology. *Geoscience Frontiers*, **7**, 581–589.

Sugden, T., Deb, M. & Windley, B. 1990. The tectonic setting of mineralisation in the Proterozoic Aravalli Delhi Orogenic belt, NW India. *Developments in Precambrian Geology*, **8**, 367–390.

Torsvik, T., Carter, L., Ashwal, L., Bhushan, S., Pandit, M. & Jamtveit, B. 2001. Rodinia refined or obscured: palaeomagnetism of the Malani igneous suite (NW India). *Precambrian Research*, **108**, 319–333.

Tucker, R., Ashwal, L. & Torsvik, T. 2001. U–Pb geochronology of Seychelles granitoids: a Neoproterozoic continental arc fragment. *Earth and Planetary Science Letters*, **187**, 27–38.

Vermeesch, P. 2012. On the visualisation of detrital age distributions. *Chemical Geology*, **312–313**, 190–194.

Wang, L.J., Yu, J.H., Griffin, W.L. & O'Reilly, S.Y. 2012. Early crustal evolution in the western Yangtze Block: Evidence from U–Pb and Lu–Hf isotopes on detrital zircons from sedimentary rocks. *Precambrian Research*, **222–223**, 368–385.

Wang, W. & Zhou, M.-F. 2012. Sedimentary records of the Yangtze Block (South China) and their correlation with equivalent Neoproterozoic sequences on adjacent continents. *Sedimentary Geology*, **265–266**, 126–142.

Wang, W. & Zhou, M.F. 2014. Provenance and tectonic setting of the Paleo- to Mesoproterozoic Dongchuan Group in the southwestern Yangtze Block, South China: implication for the breakup of the supercontinent Columbia. *Tectonophysics*, **610**, 110–127.

Wang, W., Cawood, P.A., Zhou, M.-F. & Zhao, J.-H. 2016. Palaeoproterozoic magmatic and metamorphic events link Yangtze to northwest Laurentia in the Nuna supercontinent. *Earth and Planetary Science Letters*, **433**, 269–279.

Wang, X.L., Zhou, J.C., Qiu, J.S., Zhang, W.L., Liu, X.M. & Zhang, G.L. 2006. LA-ICP-MS U–Pb zircon geochronology of the Neoproterozoic igneous rocks from Northern Guangxi, South China: Implications for tectonic evolution. *Precambrian Research*, **145**, 111–130.

Wiedenbeck, M. & Goswami, J.N. 1994. High precision $^{207}Pb/^{206}Pb$ zircon geochronology using a small ion microprobe. *Geochimica et Cosmochimica Acta*, **58**, 2135–2141.

Wiedenbeck, M., Goswami, J.N. & Roy, A.B. 1996. Stabilization of the Aravalli Craton of northwestern India at 2.5 Ga: An ion microprobe zircon study. *Chemical Geology*, **129**, 325–340.

Wilde, S., Valley, J., Peck, W. & Graham, C. 2001. Evidence from detrital zircons for the existence of continental crust and oceans on the Earth 4.4 Gyr ago. *Nature*, **409**, 175–178.

Wu, F.Y., Yang, Y.H., Xie, L.W., Yang, J.H. & Xu, P. 2006. Hf isotopic compositions of the standard zircons and baddeleyites used in U–Pb geochronology. *Chemical Geology*, **234**, 105–126.

Xing, X., Wang, Y. & Zhang, Y. 2016. Detrital zircon U–Pb geochronology and Lu–Hf isotopic compositions of the Wuliangshan metasediment rocks in SW Yunnan (China) and its provenance implications. *Journal of Earth Science*, **27**, 412–424.

Yu, J.H., O'Reilly, S.Y. *et al.* 2008. Where was South China in the Rodinia supercontinent?: Evidence from U–Pb geochronology and Hf isotopes of detrital zircons. *Precambrian Research*, **164**, 1–15.

Yu, J.H., O'Reilly, S.Y., Zhou, M.F., Griffin, W.L. & Wang, L.J. 2012. U–Pb geochronology and Hf–Nd isotopic geochemistry of the Badu Complex, Southeastern China: Implications for the Precambrian crustal evolution and paleogeography of the Cathaysia Block. *Precambrian Research*, **3–4**, 347–363.

Zhao, G.C., Cawood, P.A., Wilde, S.A. & Sun, M. 2002. Review of global 2.1–1.8 Ga orogens: implications for a pre-Rodinia supercontinent. *Earth-Science Reviews*, **59**, 125–162.

Zhao, G.C., Li, S.Z., Sun, M. & Wilde, S.A. 2011*a*. Assembly, accretion, and break-up of the Palaeo-Mesoproterozoic Columbia supercontinent: record in the North China Craton revisited. *International Geology Review*, **53**, 1331–1356.

Zhao, J.H. & Zhou, M.F. 2007. Geochemistry of Neoproterozoic mafic intrusions in the Panzhihua district (Sichuan Province, SW China): Implications for subduction-related metasomatism in the upper mantle. *Precambrian Research*, **152**, 27–47.

Zhao, J.H., Zhou, M.F., Yan, D.P., Zheng, J.P. & Li, J.W. 2011*b*. Reappraisal of the ages of Neoproterozoic strata in South China: no connection with the Grenvillian orogeny. *Geology*, **39**, 299–302.

Zhao, X.F., Zhou, M.F., Li, J.W., Sun, M., Gao, J.F., Sun, W.H. & Yang, J.H. 2010. Late Paleoproterozoic to early Mesoproterozoic Dongchuan Group in Yunnan, SW China: Implications for tectonic evolution of the Yangtze Block. *Precambrian Research*, **182**, 57–69.

Zheng, Y.F. 2004. Position of South China in configuration of Neoproterozoic supercontinent. *Chinese Science Bulletin*, **49**, 751–753.

Zheng, Y.F., Wu, R.X., Wu, Y.B., Zhang, S.B., Yuan, H. & Wu, F.Y. 2008. Rift melting of juvenile arc-derived crust: Geochemical evidence from Neoproterozoic volcanic and granitic rocks in the Jiangnan Orogen, South China. *Precambrian Research*, **163**, 351–383.

Zhong, Y., Zhai, M., Peng, P., Santosh, M. & Ma, X. 2015. Detrital zircon U–Pb dating and whole-rock geochemistry from the clastic rocks in the northern marginal basin of the North China Craton: Constraints on depositional age and provenance of the Bayan Obo Group. *Precambrian Research*, **258**, 133–145.

Zhou, M.F., Yan, D.P., Wang, C.L., Qi, L. & Kennedy, A. 2006. Subduction-related origin of the 750 Ma Xuelongbao adakitic complex (Sichuan Province, China): Implications for the tectonic setting of the giant Neoproterozoic magmatic event in South China. *Earth and Planetary Science Letters*, **248**, 286–300.

Zhou, M.F., Zhao, X.F., Chen, W.T., Li, X.C., Wang, W., Yan, D.P. & Qiu, H.N. 2014. Proterozoic Fe–Cu metallogeny and supercontinental cycles of the southwestern Yangtze Block, southern China and northern Vietnam. *Earth-Science Reviews*, **139**, 59–82.